

GENOMES UNCOUPLED1 plays a key role during the de-etiolation process in Arabidopsis

Authors/Affiliations: Tamara Hernández-Verdeja^{1,2*}, Linda Vuorijoki¹, Xu Jin¹, Alexander Vergara¹, Carole Dubreuil¹ and Åsa Strand^{1*}

¹Umeå Plant Science Centre, Department of Plant Physiology, Umeå University, Umeå, SE 901 87, Sweden

Additional Footnotes: ²Current address: Lancaster Environment Centre, Lancaster University, Lancaster, LA1 4YQ, UK.

Correspondence: *Åsa Strand and Tamara Hernández-Verdeja

Email: asa.strand@umu.se, t.hernandez-verdeja@lancaster.ac.uk

Received: 14 February 2022

Accepted: 14 March 2022

ORCID

Tamara Hernández-Verdeja 0000-0002-2148-3676

Linda Vuorijoki 0000-0003-2435-9598

Åsa Strand 0000-0001-6664-0471

This article has been accepted for publication and undergone full peer review but has not been through the copyediting, typesetting, pagination and proofreading process, which may lead to differences between this version and the [Version of Record](#). Please cite this article as [doi: 10.1111/NPH.18115](https://doi.org/10.1111/NPH.18115)

This article is protected by copyright. All rights reserved

Summary

- One of the most dramatic challenges in the life of a plant occurs when the seedling emerges from the soil and exposure to light triggers expression of genes required for establishment of photosynthesis.
- This process needs to be tightly regulated as premature accumulation of light harvesting proteins and photoreactive chlorophyll precursors cause oxidative damage when the seedling is first exposed to light. Photosynthesis genes are encoded by both nuclear and plastid genomes and to establish the required level of control, plastid-to-nucleus (retrograde) signalling is necessary to ensure correct gene expression.
- We herein show that a negative GUN1-mediated retrograde signal restricts chloroplast development in darkness and during early light response by regulating the transcription of several critical TFs linked to light response, photomorphogenesis, and chloroplast development, and consequently their downstream target genes in Arabidopsis.
- Thus, the plastids play an essential role during skotomorphogenesis and the early light response and GUN1 acts as a safeguard during the critical step of seedling emergence from darkness.

Keywords: chloroplast, greening, plastid retrograde signalling, GUN1, light signalling, transcriptional regulation

Introduction

Establishment of photosynthesis through chloroplast biogenesis is a highly regulated and complex process. It is light regulated and under nuclear control as chloroplast biogenesis starts by activation of the phytochromes leading to degradation of the PHYTOCHROME-INTERACTING FACTORS (PIFs), the major transcriptional repressors of development in light, and massive nuclear transcriptional changes (Jiao *et al.*, 2005; Leivar & Monte, 2014). Light triggers the first phase of chloroplast development characterized by an increased expression of the photosynthesis associated nuclear genes (*PhANGs*) (Dubreuil *et al.*, 2018; Yang *et al.*, 2019; Yoo *et al.*, 2019). This initial response is believed to be completely under nuclear control, but the second phase of development required to establish fully photosynthetically active chloroplasts depends upon a retrograde signal originating in the plastids (Dubreuil *et al.*, 2018). The nature of this signal has been intensively sought after but has so far remained unknown. Paramount to the discovery of the

existence of retrograde signals was the identification of *GENOMES UNCOUPLED* (*GUN*) genes, which link the developmental and physiological status of the chloroplasts with expression of nuclear genes (Susek *et al.*, 1993). Among the *GUN* genes, *GUN1* has attracted the most attention as it has been proposed to integrate several signals associated with plastid dysfunction, specifically those induced by inhibitors of chloroplast development like norflurazon or lincomycin (Sullivan & Gray, 1999; Koussevitzky *et al.*, 2007; Tadini *et al.*, 2016, 2020b; Llamas *et al.*, 2017; Hernández-Verdeja & Strand, 2018; Wu *et al.*, 2018, 2019a; Zhao *et al.*, 2019; Marino *et al.*, 2019; Shimizu *et al.*, 2019). Although *GUN1* contains domains often associated with RNA-binding (Koussevitzky *et al.*, 2007), a direct role in plastid RNA metabolism has never been confirmed, and *GUN1* has rather been associated with other processes in the plastids, such as maintenance of chloroplast protein homeostasis, regulation of protein import, plastid RNA editing, plastid transcription, and tetrapyrrole biosynthesis through the interaction with several different plastid proteins (Tadini *et al.*, 2016, 2020b; Llamas *et al.*, 2017; Wu *et al.*, 2018, 2019a; Marino *et al.*, 2019; Shimizu *et al.*, 2019; Zhao *et al.*, 2019). Despite all these efforts, neither the biologically relevant function of *GUN1*, nor the nature of the *GUN1*-derived signal, whether it is positive or negative, has been determined.

Emerging from darkness is a delicate balancing act and recent reports have highlighted the importance of repressive mechanisms, both at the transcriptional and post-transcriptional level, to block premature chloroplast development in the dark, and to avoid over-accumulation of phototoxic photosynthetic products (Armarego-Marriott *et al.*, 2020). These repressive processes are largely controlled by the PIFs and the degradation of transcriptional regulators by the ubiquitin-proteasome (COP/DET/FUS) pathway (Seluzicki *et al.*, 2017). In addition, the brassinosteroid responsive BRASSINAZOLE-RESISTANT 1 (BZR1) transcription factor has been reported to interact with PIF4 and form a module to control gene expression during skotomorphogenesis (Oh *et al.*, 2012). The gibberellin-regulated DELLA transcriptional regulators are present in etiolated cotyledons and also interact with the PIFs and thereby regulate the expression of the PIF target genes, such as genes encoding proteins involved in chlorophyll biosynthesis and other photosynthetic proteins (Cheminant *et al.*, 2011).

In addition to the light-induced nuclear control, retrograde signalling is required for chloroplast biogenesis and early studies indicated that a plastid signal pre-exist in dark or is rapidly generated

in response to light (Sullivan & Gray, 1999). One of the first phenotypes described for *gun1* was reduced greening and survival of dark-grown seedlings shifted to light (Susek *et al.*, 1993), a phenotype probably linked to the high accumulation of protochlorophyllide (Pchl) in the dark-grown *gun1* mutants (Xu *et al.*, 2016; Shimizu *et al.*, 2019). The increased Pchl and impaired de-etiolation of *gun1* mutants have been well described but these phenotypes, and their implications for the GUN1-dependent retrograde signal, have not been properly investigated. To gain insight into the actual physiological role of the GUN1-mediated retrograde signal during chloroplast biogenesis and to explore a possible role of the plastids during skotomorphogenesis and early light response, we set our research focus on the dark-grown plastid forms, etioplasts, and proplastids. This approach revealed that GUN1 is already present both in proplastids and etioplasts, and that GUN1 protein levels decrease in light and as chloroplast development progresses. We performed an RNA-Seq analysis to show that the GUN1-mediated signal regulates nuclear gene expression already in the dark, before the onset of chloroplast development and during the early light response in the absence of any chemical or genetically induced plastid stress. GUN1 contributes to the fine-tuning of nuclear gene expression in dark and during early light response, and thus acts as a safeguard during the critical developmental stage of greening.

Materials and Methods

Plant Material

Arabidopsis thaliana Columbia-0 (Col-0) and the T-DNA insertion mutants, *gun1-102* (SAIL_290_D09) and *gun1-103* (SAIL_742_A11) were used for all the experiments (Sun *et al.*, 2011; Dietzel *et al.*, 2015; Tadini *et al.*, 2016; Martín *et al.*, 2016). Plants were genotyped to confirm the T-DNA insertions and identify homozygous individuals. Primers for genotyping are listed in Table S1. The *Arabidopsis* stable pluripotent inducible cell line has been described in Dubreuil *et al.*, 2018.

To obtain the $P_{GUN1}:GUN1:YFP$ construct the *GUN1* genomic region containing 1494 bp of the promoter was PCR-amplified using primers listed in Table S1 and cloned into pDONR207 (Invitrogen) and subcloned into pHGY binary vector (Yamaguchi *et al.*, 2008). To generate the *GUN1* artificial microRNA, primers were designed using WMD3–Web microRNA Designer and used to engineer the artificial microRNA precursor by site-directed mutagenesis using pRS300 as template (Ossowski Stephan, Fitz Joffrey, Schwab Rebecca, Riester Markus and Weigel Detlef,

personal communication; primers listed in Table S1). The amiRNA-GUN1 precursor was cloned in pDONR207 and subcloned into pMDC7 binary vector (Curtis & Grossniklaus, 2003). All constructs were verified by sequencing and transformed into *Agrobacterium tumefaciens* GV3101pM90 strain. Plants were transformed using the floral dip method (Clough & Bent, 1998) and cells as already described (Pesquet *et al.*, 2010).

Growth conditions and treatments

Seeds were surface sterilized, plated on 1x Murashige and Skoog (MS) salt mixture supplemented with vitamins (Duchefa) with 1% (w/v) sucrose, and stratified for 3 days at 4°C in darkness. For analysis with etiolated seedlings, germination was induced by exposing the seeds to white light (150 $\mu\text{mol photons m}^{-2} \text{s}^{-1}$) for 5 hours, followed by growth in darkness for 5 days at 22°C and shifted to constant white light (150 $\mu\text{mol photons m}^{-2} \text{s}^{-1}$) for the indicated times.

For greening and survival assays, at least 50 seeds per replicate were sown on 1x MS-plates with 2% (w/v) sucrose. After etiolation the seedlings were transferred to constant white light (150 $\mu\text{mol photons m}^{-2} \text{s}^{-1}$) and scored for seedlings with green open cotyledons after 48 hours, or with green true leaves after 1 week. For the evaluation of the *gun* phenotype the seedlings were grown six days under constant white light (150 $\mu\text{mol photons m}^{-2} \text{s}^{-1}$) on 1x MS plates with 2% (w/v) sucrose supplemented with 0.5 mM lincomycin hydrochloride (SIGMA L2774). For the lincomycin treatment to analyse GUN1:YFP signal in the confocal, the 1x MS media with 1% (w/v) sucrose was supplemented with 0.5 mM lincomycin hydrochloride or with distilled water as mock.

The Arabidopsis Col-0 cell culture was grown in 1x MS supplemented with 3% (w/v) sucrose and maintained in dark, 22°C, and constant shaking (Dubreuil *et al.*, 2018). Chloroplast development was induced by transferring the cells to continuous light (150 $\mu\text{mol photons m}^{-2} \text{s}^{-1}$), 22°C, MS-media with 1% (w/v) sucrose and constant shaking (Dubreuil *et al.*, 2018). For induction of *amiRNA-GUN1* the dark-grown transgenic cell lines were supplemented with 5 μM β -estradiol (Sigma E2758) or with ethanol 0.1% (v/v) as mock, after refreshing the medium and before light induction of chloroplast development. Cells were harvested by vacuum filtration at the indicated times and frozen in liquid nitrogen.

Gene expression analysis

Total RNA was isolated using Plant RNA Mini Kit (EZNA) from homogenized samples and genomic DNA was removed by DNase I treatment (Thermo-Fisher EN0525). Complementary DNA (cDNA) was synthesized using 0.5µg RNA with iScript cDNA Synthesis kit (Bio-Rad 1708891) according to the manufacturer's instructions and 10x diluted. Real-time PCR was performed using iQSYBR Green Supermix (Bio-Rad 1725006CUST) in a CFX96 Real-Time system (C1000 Thermal Cycler; Bio-Rad) with a two-step protocol. The primers used are listed in Table S1. All experiments were performed with four biological replicates. Relative gene expression was normalized to the expression of *ATIG13320* for seedling and *AT4G36800* for cell samples and calibrated to 1 relative to the indicated condition or genotype. Data analysis was done using CFX manager (Bio-Rad) and LinRegPCR software (Ramakers *et al.*, 2003).

RNA preparation, sequencing and data processing

Total RNA was extracted from whole seedlings using RNeasy Plant Kit (Qiagen). The quantity and quality of the RNA was determined both by Nanodrop 2000 (Thermo Scientific) and Plant RNA Nano assay (v.1.3) built in Agilent 2100 Bioanalyzer System according to RNA 6000 Nano kit protocol (Agilent Technologies, Waldbronn, Germany). Samples were sequenced by Beijing Genomics Institute (BGI) using the DNBSEQ platform, obtaining an average yield of 4.93G data per sample. Adaptor contamination, rRNA, low-quality and reads with too many N bases were removed by SOAPnuke (Chen *et al.*, 2018). The RNA-Seq reads filtering summary is in Table S2. Clean reads were aligned against TAIR 10.1 GCF_000001735.4 reference genome using Bowtie2 v2.2.5 (Langmead & Salzberg, 2012). Gene expression levels were quantified by RSEM v1.2.12 (Li & Dewey, 2011). Normalized gene expression levels, calculated by variance stabilizing transformation (VST), and differential expressed genes (DEGs) using q-value ≤ 0.05 as threshold were obtained with DESeq2 (Love *et al.*, 2014). Volcano plots showing significant DEGs are available in Supplementary data Fig. S1. DEGs were ranked by fold change for further analysis.

Gene regulatory network and functional analysis

The Gene Regulatory Network (GRN) was built using TF2Network using positive co-expression values and motifs overrepresented on promoters of DEGs (Kulkarni *et al.*, 2018). Only DEGs were considered to build the network, and all Transcription Factors (TFs) that were not DEGs were removed of the GRN. TFs and its associated families were obtained from PlantTFDB (Jin *et*

al., 2014). Network visualization was done with Cytoscape (Shannon *et al.*, 2003). Gene Ontology (GO) enrichment analyses were performed with standalone version of GeneMerge (Castillo-Davis & Hartl, 2003). REVIGO was used to summarize and reduce GO terms (Supek *et al.*, 2011). Prediction of subcellular localization was done with SUBA4 (Hooper *et al.*, 2017).

Transcriptomic data for comparisons were obtained from Martín *et al.*, 2016 (GSE78969), Koussevitzky *et al.*, 2007 (GSE5770), Wu *et al.*, 2018 (GSE122667), Waters *et al.*, 2009 and Ni *et al.*, 2017. Venn diagrams were done with Venny (Oliveros, 2015).

Protochlorophyllide determination

50 seedlings grown in the dark for 5 days were harvested under dim green light and frozen in liquid nitrogen. Pigments were extracted by mixing the homogenized material in ice-cold 80% buffered acetone and incubation at 4°C in the dark overnight. Cell debris was removed by centrifugation at 4°C for 20 min at 14000 g. The fluorescence emission spectra were obtained using a JASCO FP-6500 spectrofluorometer with an excitation wavelength of 440 nm, bandwidth 5 nm, and emission recorded between 600-700 nm, bandwidth 5 nm.

Anthocyanin accumulation

To observe anthocyanin production we used the method described in Cottage *et al.*, 2010. Briefly, the seeds were sterilized and sown in 1x MS with 2% sucrose supplemented with 0.5 mM lincomycin, stratified for 2 days at 4°C in darkness and then grown at 22°C in constant white light (100 $\mu\text{mol photons m}^{-2} \text{s}^{-1}$) for 4 days.

Confocal microscopy and quantification of fluorescence

Confocal laser-scanning microscopy was performed with an inverted Carl-Zeiss LSM880 system equipped with a Plan-Apochromat 10x/0.45 M27 objective (numerical aperture: 0.45; Carl Zeiss) or a C-Apochromat 40x/1.2 W Korr FCS M27 objective (numerical aperture: 1.20; Carl Zeiss). YFP detection was done using an excitation 514 nm wavelength laser and a 517-606 nm filter. CFP detection was done using an excitation 405 nm laser and a 415-505 nm filter. Chlorophyll autofluorescence was detected using an excitation 633 nm laser and 638-721 nm filter.

The quantification of GUN1:YFP signal was done with high resolution images (2048x2048 pixels) of chloroplast captured with the C-Apochromat 40x/1.2 W Korr FCS M27 objective. Raw confocal images were analysed using Fiji processing image package (Schindelin *et al.*, 2012). Circular brightest areas, 40 or 30 pixels in radius, within plastids of cotyledons or roots, respectively, were selected for the quantification of the fluorescence pixel intensity (Mean Grey Value tool in Fiji). The cotyledons were separated in etiolated seedlings to enable visualization and quantification of the signal. Only the central part of the cotyledons, corresponding to the spongy mesophyll cells, and the epidermis layer of the root tips were selected for the images used for the quantification. The quantification of GUN1:YFP in roots was performed on the epidermis layer of the root tips. Fifteen to twenty chloroplasts were measured per cotyledon, and nine to fifteen cotyledons were analysed for each of the three independent biological replicates. Fifteen plastids per root were measured from three to five roots.

Statistical analyses

Statistics were done using R 3.6.0 (R Core Team, 2019), Rstudio 1.0.136 (RStudio Team, 2016), *FSA* (Ogle *et al.*, 2019), and *rcompanion* (Mangiafico, 2019). Box-plots were done with BoxPlotR (<http://shiny.chemgrid.org/boxplotr/>). Heatmaps and bubble plots were done with ggplot (Wickham, 2016).

Results

GUN1 is present in proplastids and regulates expression of *PhANGs*

GUN1 is a very low abundant protein, but using a GUN1 35S driven overexpression line, it has been detected in cotyledons of light-grown *Arabidopsis* seedlings (Wu *et al.*, 2018). To investigate GUN1 activity isolated from the plant developmental program, we monitored levels of GUN1 during light-induced greening of a pluripotent *Arabidopsis* single cell culture. In this cell culture chloroplast development proceeds from proplastids to functional chloroplasts similarly to the process taking place in the meristems to form mature leaves. In the cell culture the greening process is significantly slower compared to the process in light exposed etiolated seedlings and the development of a mature functional chloroplast from the proplastids takes several days (Dubreuil *et al.*, 2018). The cell line does however provide both high temporal and cellular resolution. We transformed the *Arabidopsis* cells with *GUN1:YFP* under the control of the *GUN1* endogenous promoter ($P_{GUN1}:GUN1:YFP$) and analysed GUN1:YFP localization in two independent lines. To

confirm plastid localization we used PEND:CFP, a marker for plastid nucleoids (Terasawa & Sato, 2005; Kindgren *et al.*, 2012a). Surprisingly, the confocal microscopy revealed that GUN1:YFP fluorescence is present in the proplastids of dark-grown transgenic cells (Fig. 1a; Fig. S2a). A clear fluorescence signal was detected both from the dark-grown cells and the cells exposed to light for 1 and 5 days. The GUN1:YFP signal completely overlapped with the plastid marker confirming a sole plastid localization of GUN1 under these conditions (Fig. 1a), and chlorophyll autofluorescence is first detected at day 5 indicating that the proplastids initiated the transition to photosynthetically functional chloroplasts (Fig. 1a; Fig. S2a). The cell images also clearly show movement of the plastids in response to light and the proplastids cluster around the nucleus following light exposure (Fig. 1a) (Dubreuil *et al.*, 2018).

The $P_{GUN1}:GUN1:YFP$ cell lines clearly show that the GUN1 protein is present in proplastids and in the dark. To investigate the possibility that a GUN1-dependent retrograde signal is active in the proplastids we analysed expression of two known retrograde-responsive *PhANGs* in the cell culture, *LHCB1.1* and *LHCB2.4*. We generated independent transgenic cell lines with an estradiol-inducible artificial microRNA (*amiGUN1*) to reduce *GUN1* expression (Fig. S2b). *LHCB1.1* and *LHCB2.4* showed higher expression levels in the estradiol-treated *amiGUN1* dark-grown cells and maintained higher expression during the early light response compared to the mock-treated *amiGUN1* cells in both lines (Fig. 1b; Fig. S2c). The presence of GUN1 and the higher expression of *LHCB* genes in the *amiGUN1* lines support a role for GUN1 and the GUN1 retrograde signal controlling nuclear gene expression in proplastids and during the chloroplast development process.

GUN1 is present in etioplasts and plastids of non-green plant tissues

The existence of a retrograde signal in dark-grown plants has been suggested by several studies (Sullivan & Gray, 1999; Woodson *et al.*, 2013; Martín *et al.*, 2016) and our new results demonstrating GUN1 presence and activity in proplastids, encouraged us to investigate GUN1 also in etiolated seedlings. We analysed the levels of GUN1 protein in dark-grown seedlings and during de-etiolation, using Arabidopsis *gun1-102* and *gun1-103* mutants complemented with the same construct used in cell culture, $P_{GUN1}:GUN1:YFP$ (*gun1-102 GUN1:YFP* and *gun1-103 GUN1:YFP*), which allowed us to monitor GUN1 in seedlings under natural conditions. Independent transformed mutant lines recovered the wild-type phenotype regarding accumulation of anthocyanins in 4d-old seedlings (Cottage *et al.*, 2010) and wild-type expression of *LHCB2.2*

and *LHCB2.4* upon lincomycin treatment (Koussevitzky *et al.*, 2007) confirming that the GUN1:YFP fusion protein was functional (Fig. S3). The dynamics of GUN1:YFP accumulation during the de-etiolation process was determined by confocal microscopy. A strong YFP fluorescence signal was detected in etioplasts of cotyledons from 5d-old dark-grown seedlings in all the complemented lines (Fig. S4a), indicating that GUN1 is present in non-photosynthetic plastids before light-induced differentiation. Following 24h light exposure the GUN1:YFP signal decreased and the GUN1 levels were almost undetectable (Fig. S4a). Expression of the transgene was detected with qPCR, indicating that the decrease in the fluorescence signal after 24h in light is not due to reduced *GUN1:YFP* expression. The expression profile of the GUN1:YFP transgene is similar to the endogenous *GUN1* during the dark to light shift (Fig. S4b,c). Furthermore, in contrast to the observation at the protein level, the expression of *GUN1* increased in response to light. To further investigate the dynamics of the GUN1 protein, a more detailed study was performed using two complemented lines, *gun1-103 GUN1:YFP #6.3.6* and *gun1-102 GUN1:YFP #6.1.1*. We analysed the GUN1 fluorescence signal over time following a shift of 5d-old etiolated seedlings to constant light. Fluorescence could be detected in the cotyledons following 1 and 3 hours exposure to light for but the levels were slightly lower compared to the dark. The GUN1 fluorescence signal further declined following 6 hours and reached the lowest level after 24h in the light when the cotyledons were green and chloroplast developed (Fig. 2a,b; Fig. S5a,b). We performed an immunoblot blot analysis using cotyledons of *gun1-103 GUN1:YFP* from the time course experiment. The Western blot results displayed a similar pattern to the quantification of the fluorescence signal, with high GUN1:YFP protein levels in the etiolated cotyledons that decrease with light and progression of chloroplast development (Fig. S6: Methods S1). A second band of larger size appeared at the later time points (Fig. S6). This was also observed by Wu *et al* 2018, but the significance of this band is at this point unclear.

Degradation of GUN1 upon chloroplast development in light was consistent with the report using a *P_{35S}:GUN1:GFP* line, showing that the GUN1 protein is highly unstable and that its degradation might be controlled by the CLPC chaperone (Wu *et al.*, 2018). In contrast, GUN1:YFP levels in plastids of the root tissues remained high during the entire de-etiolation process further indicating that the GUN1 signal is active in non-photosynthetic plastids independent of light (Fig. 2c,d; Fig. S5c,d). The detection of elevated levels of the GUN1:YFP fusion protein in etioplasts and in root plastids, indicates that GUN1-dependent retrograde signal is active before the onset of chloroplast

biogenesis in seedlings and that the degradation of GUN1 might be triggered by chloroplast biogenesis in photosynthetic tissues.

The GUN1 retrograde signal regulates nuclear gene expression in etiolated seedlings

Until this date, most transcriptomic profiling of *gun1* mutants has been done on light grown seedlings where chloroplast development has already been completed and GUN1 protein is at very low levels, or under conditions that block chloroplast development such as growth on inhibitors like lincomycin or norflurazon (Koussevitzky *et al.*, 2007; Marino *et al.*, 2019; Wu *et al.*, 2019b; Richter *et al.*, 2020). Our results suggest that GUN1 could contribute to the suppression of plastid development by controlling nuclear gene expression. In order to reveal the extent of GUN1-dependent control of nuclear gene expression in etiolated seedlings and during early light response we performed RNA-Seq analysis of *gun1-102* and wild-type 5d-old etiolated seedlings (D 0h), and 5d-old etiolated seedlings subsequently exposed to light for 3h (L 3h) or 24h (L 24h). This allowed us to analyse the effect of GUN1 in etiolated seedlings when GUN1 levels are very high, during early light induction of chloroplast development when the levels are still high, and when chloroplast development is completed and GUN1 levels are at a minimum. In agreement with our observed protein data the largest number of differentially expressed genes (DEGs, q -value ≤ 0.05 , Fig. **S1**) in *gun1-102* compared to wild-type was observed in etiolated seedlings with 4425 DEGs (2463 up-regulated and 1962 down-regulated genes), followed by seedlings exposed to 3h light with 3323 DEGs (2101 up-regulated and 1222 down-regulated genes). In comparison the number of DEGs after 24h in light was 371 (271 up-regulated and 100 down-regulated), which reflects the low levels of GUN1 following 24 h light exposure (Fig. **3a**; Table **S3**).

To identify specific genes that depend upon GUN1, we compared the DEGs for the three conditions (D 0h, L 3h and L 24h). Overlapping DEGs showed a significant number of both shared and specific genes between the three time-points (Fig. **3b**). In total, 38% of the genes were exclusively deregulated in etiolated seedlings (Dark), 40% were common to both etiolated and de-etiolated seedlings (Dark-Light), and 22% were differentially expressed only in seedlings exposed to light (Light). These results again support an important role of GUN1 in etioplasts, and during the transition from dark to light.

A detailed SUBA4-analysis of the predicted subcellular localization of the proteins encoded by the DEGs in each group revealed a large percentage of plastid localized proteins (Fig. 3c). The percentage of plastid proteins was high in the dark, and decreased with time in light. The GO enrichment analysis for the up- and down-regulated genes in *gun1-102* at D 0h and L 3h also showed a significant number of plastid related terms, especially in D 0h up-regulated DEGs where genes linked to chloroplast membrane, thylakoid membrane and envelope, and photosystem I were enriched (Fig. 4a; Fig. S7a; Table S4). A detailed search revealed several up-regulated *LIGHT HARVESTING CHLOROPHYLL A/B* genes (e.g. *LHCB1.3*, *LHCB 2.1*, *LHCB2.2*, *LHCB2.4*, *LHCB4.2* and *LHCB3*), and a specific up-regulation in D 0h of photosystem I (PSI) and II (PSII) assembly factors like *ALBINO 3* and *PIGMENT DEFECTIVE 149*, and *PSA2* (Fristedt *et al.*, 2014; Schneider *et al.*, 2014). Accordingly, many PSI (e.g. *PSAO*, *PSAF*, *PSAH*, *PSAE*, *PSAH-1*, *PSAL*, *PSAE-1*) and PSII (e.g. *PSBP-1*, *NPQ4*, *PSBR*, *PnsL2*, *PSBY*, *PSBX*, *PSBO1*, *PSBO2*, *PSBQ-2*) subunits were up-regulated in the *gun1-102* mutant in D 0h. Among the other enriched categories in the up-regulated genes were GO terms related to plant development (e.g. *BRZ-INSENSITIVE-LONG HYPOCOTYLS 4*, *DWARF IN LIGHT 1*) and response to light (e.g. *PIF1*, 4 and 8, *PHYB ACTIVATION TAGGED SUPPRESSOR 1*, *FAR-RED-ELONGATED HYPOCOTYLI-LIKE*, and *KIDARI*), and in the down-regulated genes there was an enrichment for plastid and thylakoid membranes (e.g. *VARIEGATED2*, *CHLOROPLAST PROTEIN-ENHANCING STRESS TOLERANCE*, and *FLUORESCENT IN BLUE LIGHT*), protein folding, and translation (e.g. *CHAPERONIN 60 BETA*, *CHLOROPLAST HEAT SHOCK PROTEIN 70-1*, *CR88/HSP90.5*, *TRANSLOCON AT THE OUTER ENVELOPE MEMBRANE OF CHLOROPLASTS 33* and *159*, *HSP93-III/CLPC2*, *EUKARYOTIC TRANSLATION INITIATION FACTOR 3C*, *3B-1* and *3B-2*) (Fig. 4; Fig. S7b, Table S4). The GO terms enriched in the RNA-Seq dataset reflect described targets for the GUN1 retrograde signal in response to plastid stress repressing chloroplast development, antagonizing the light development pathways, and regulating protein homeostasis, with the novelty that this response is present in dark grown etiolated seedlings.

GUN1-mediated and lincomycin triggered retrograde signals partially overlap

GUN1 is well characterized to play an important role in response to plastid stress conditions (Koussevitzky *et al.*, 2007; Tadini *et al.*, 2016, 2020b; Llamas *et al.*, 2017; Wu *et al.*, 2018, 2019a; Marino *et al.*, 2019; Shimizu *et al.*, 2019; Zhao *et al.*, 2019), conditions that are also shown to

block GUN1 degradation (Wu *et al.*, 2018). We used lincomycin, an inhibitor of plastid translation, to test if GUN1 levels were affected in etiolated and de-etiolated seedlings using our mutant lines complemented with *GUN1:YFP*. A strong fluorescence signal was detected in the presence of lincomycin in etiolated and de-etiolated *gun1-103 GUN1:YFP #6.3.6* and *gun1-102 GUN1:YFP #6.1.1* seedlings (Fig. **5a,b**; Fig. **S8a,b**). The GUN1:YFP levels in the lincomycin-treated seedlings were significantly higher compared to the non-treated seedlings confirming that lincomycin-induced plastid stress blocks GUN1 degradation even in the dark (Fig. **5a,b**; Fig. **S8a,b**).

Retrograde signals induced by lincomycin are known to repress *PhANGs*, a repression that has been reported to be mainly mediated by GUN1 (Koussevitzky *et al.*, 2007). We analysed GUN1- and lincomycin-mediated transcriptomic profiles using previously published data (Koussevitzky *et al.*, 2007; Martín *et al.*, 2016; Wu *et al.*, 2019b). The comparison of the DEGs up-regulated in *gun1-102* D 0h with up-regulated DEGs in the lincomycin light-grown *gun1* seedlings and down-regulated DEGs in lincomycin light-grown wild-type seedlings revealed a relevant overlap, with 241 (9.8%) and 217 (8.8%) common DEGs, respectively (Fig. **5c**). To avoid potential differences due to light signalling, we compared our data with down-regulated DEGs in etiolated wild-type seedlings to wild-type seedlings treated with lincomycin. The results were similar and an overlap of 115 DEGs (less than 5%) was observed with the up-regulated DEGs in *gun1-102* D 0h (Fig. **5c**). When the comparisons were made with our data for up-regulated DEGs in *gun1-102* L 3h the overlap was smaller (Fig. **S8c**). The shared DEGs at all the different comparisons showed enrichments in the GO terms related to photosynthesis (Table **S5**), and among them we found *GLK1* and GLK targets (Table **S6**). This is in agreement with the described role of GUN1 to repress *PhANGs* via GLK1 when chloroplast development is impaired (Kakizaki *et al.*, 2009; Martín *et al.*, 2016; Tokumaru *et al.*, 2017). Taken together, our results suggest that there are common and exclusive pathways for GUN1 and lincomycin signals.

The GUN1 retrograde signal controls the expression of a large number of transcription factors during the de-etiolation process

Among the DEGs obtained by comparing *gun1-102* with wild-type plants in dark 0h and light 3h there was a high percentage of genes encoding nuclear localized proteins (Fig. **3c**). The GO cellular component term “nucleus” was enriched for all the DEGs, and the GO term “transcription

regulatory region sequence-specific DNA binding” was enriched in the up-regulated genes in both D 0h and L 3h (Fig. 4; Fig. S7), suggesting that the expression of transcriptional regulators was affected. So far only a few transcription factors have been described to respond to the GUN1 retrograde signal (Kakizaki *et al.*, 2009; Richter *et al.*, 2020). Two of them are the GLKs, major regulators of chloroplast biogenesis. In our transcriptomics profile of *gun1-102*, only *GLK1* was up-regulated at the three time points, confirming previous reports indicating that the GUN1 retrograde signal primarily regulates *GLK1* expression, and not *GLK2* (Martín *et al.*, 2016). We used available transcriptomic data for the GLKs (Waters *et al.*, 2009; Ni *et al.*, 2017) to search for potential GLK-downstream genes in our data set. There is a small overlap between the genes induced by the GLKs and the up-regulated DEGs in *gun1-102* at D 0, L 3 and 24h. In total, only 15% of the DEGs in *gun1-102* are also under GLK control (Fig. S9).

It has been reported that GUN1 promote anthocyanin biosynthesis in response to inhibitors of plastid biogenesis through the regulation of several *MYBs* and potentially of *ELONGATED HYPOCOTYL 5 (HY5)* (Ruckle & Larkin, 2009; Richter *et al.*, 2020). In line with these results, we found expression of *MYB12* and *HY5* to be down-regulated in *gun1-102* in L 3h, but only two early anthocyanin biosynthesis genes were down-regulated in the mutant (PHENYLALANINE AMMONIA LYASE and 4-COUMAROYL COA LIGASE) (Fig. S10a). Together with *GLKs*, the *MYB12* and *HY5* represent the few already suggested targets of the GUN1 signal.

To investigate the possibility that GUN1 is regulating other transcription factors than what has been reported in the literature, we screened our dataset and found 308 transcription factors deregulated in *gun1-102*, mainly in D 0h and L 3h, which is in accordance with the higher number of DEGs at these two time points (Fig. S10a). GO enrichment, excluding terms related to transcription, indicated that these transcriptional regulators were involved in response to hormones, light, abiotic factors and development (Fig. S10b). Among the TFs down-regulated in *gun1-102* we found the already mentioned *MYB12* and *HY5*, but also *REPRESSOR OF GA1-3 1 (RGA1)* a DELLA protein that affect the activity of *HY5* and PIFs in dark (Fig. S10, Fig. S11) (Alabadi *et al.*, 2008), *ETHYLENE INSENSITIVE3-LIKE 1 (EIL1)* that is involved in the ethylene-dependent regulation of de-etiolation (Zhong *et al.*, 2009), and *ATAF2* that is implicated in photomorphogenesis responses by regulating brassinosteroid catabolism (Peng *et al.*, 2015).

Among the up-regulated TFs in *gun1-102* were transcriptional regulators involved in de-etiolation, response to light, and other developmental processes (Fig. S10c). A detailed search identified several known transcriptional regulators associated with the transition from dark to light such as PIF1, PIF3, PIF4, PIF5, PIF8 that are major repressors of development in light and chloroplast biogenesis (Pham *et al.*, 2018), BRASSINAZOLE-RESISTANT 1 (BZR1) and BRI1-EMS-SUPPRESSOR 1 (BES1) that are involved in the brassinosteroid regulation of photomorphogenesis and repression of chloroplast development in dark (Yu *et al.*, 2011), G-BOX BINDING FACTOR 3 (GBF3) that interacts with the GLKs (Tamai *et al.*, 2002), BASIC LEUCINE ZIPPER 16 and 68 (bZIP16 and 68) that regulate *LHCB* expression and photomorphogenesis (Shaikhali *et al.*, 2012), and B-BOX DOMAIN PROTEINS 21, 24, and 25 (BBX21, 24 and 25) that regulate photomorphogenesis through the regulation of HY5 (Fig. S11) (Xu, 2020). Interestingly, a great number of these TFs were not present in the lincomycin DEGs (Fig. S12), and were only found to be mis-regulated in our *gun1-102* dataset, including *PIFs*, *BES1* and *BZR1*, and several *bZIP* involved in photomorphogenesis.

Our data reveals that loss-of-function of GUN1 results in misexpression of several key TFs associated with light signalling, response to hormones and chloroplast biogenesis during early seedling development. These data strongly suggest that the GUN1-mediated control over nuclear transcription factors during chloroplast and seedling development would be broader than previously reported.

Gene regulatory network for up-regulated TFs in *gun1-102*

Since the GUN1-dependent retrograde signal is mainly known to repress nuclear gene expression and there were a high number of TFs associated with early seedling development in the group of up-regulated TFs in *gun1-102*, we focused our efforts on these transcriptional regulators. To assess if these TFs could be involved in the GUN1 regulation and play a role in the GUN1-dependent retrograde signal we used TF2Network (Kulkarni *et al.*, 2018) and found 92 up-regulated TFs in *gun1-102* that potentially regulate the DEGs (Fig. 6). After the removal of negative co-expression values we obtained a GRN with 835 nodes, 1043 regulatory interactions, and 79 up-regulated TFs that had at least one putative binding site in promoters of the *gun1-102* DEGs (Table S7). To help visualize the most connected TFs we represented the GRN using a radial layout (Fig. 7). Among the most interconnected TFs in the inner circle were some of the TFs linked to

photomorphogenesis mentioned above like the PIFs, and BES1, and GLK1. Many of the genes encoding these TFs were up-regulated in both dark and light conditions in *gun1-102* (BES1, GLK1, PIF1, 4, and 8). When we compared the top ten up-regulated TFs in *gun1-102* with the top ten most interconnected we found three TFs C-REPEAT BINDING FACTOR 2 (CBF2), RELATED TO AP2 1 (RAP2.1), and CRYPTOCHROME-INTERACTING BASIC-HELIX-LOOP-HELIX 1 (CIB1) (Fig. 6, Fig. 7, Fig S11). None of these TFs have been directly linked to plastid signals during chloroplast development. CBF2, up-regulated in etiolated *gun1-102* seedlings, is a major regulator of cold acclimation and among its downstream genes there are chloroplasts proteins involved in thylakoid membrane protection that were de-regulated in the *gun1-102* dark 0h sample (e.g. *COLD REGULATED 314 THYLAKOID MEMBRANE 2*). Although a role for the CBFs in etiolated seedlings has not been reported, earlier work has revealed that the CBFs are regulated by plastid signals (Norén *et al.*, 2016). RAP2.1, which was found to be up-regulated in dark 0h and light 3h, has been described as a repressor of abiotic stress responses regulating the expression of response genes like some *COLD REGULATED* genes (Dong & Liu, 2010). CIB1, up-regulated only in light 3h, is involved in flowering in response to blue light by interacting with CRY2 and CO (Liu *et al.*, 2018). Taken together, our results from the RNA-Seq analysis strongly indicate that the GUN1 retrograde signal regulates a large number of TFs, beyond the already described GLK1, to control nuclear gene expression before the onset of light and during the first hours of light response.

Discussion

Emerging from darkness is a dangerous task for seedlings, as the levels of chlorophyll binding proteins, and chlorophyll intermediates must be carefully controlled to provide sufficient material to build the photosynthetic machinery, while avoiding a lethal oxidative burst that results from the overaccumulation of these components when the seedling is exposed to light (op den Camp *et al.*, 2013; Liu *et al.*, 2017). We herein show that plastids play a major part in controlling this dangerous process through a negative GUN1-mediated retrograde signal which restricts chloroplast development by regulating the transcription of several critical TFs linked to light response, photomorphogenesis, and chloroplast development, and consequently their downstream target genes (Fig. 8). Based on our data we present a model where the GUN1-mediated retrograde signal is active before light-triggered chloroplast biogenesis and without any plastid impairment. We found GUN1 i) to be present in the dark, ii) to control expression of transcriptional regulators,

which further iii) affect the expression of downstream photosynthesis related genes in both seedlings and in cell lines mimicking meristematic cells, and iv) prevent premature chloroplast development and seedling damage. Our results strongly indicate that GUN1 has a protective role and is clearly active before the transition to photoautotrophy in response to light.

In darkness, a complex network of transcriptional regulators, such as the PIFs, EIN3/EIL1, BZR1/BES1 and DELLA proteins, repress chloroplast development and photomorphogenesis (Hernández-Verdeja *et al.*, 2020). Light-activation of phytochromes lifts this repression, and generates an induction of the *GLK* genes and stabilization of the transcription factor HY5 leading to the first nuclear transcriptional changes that give rise to chloroplast development and de-etiolation (Jiao *et al.*, 2007; Leivar & Monte, 2014). In response to plastid stress, the GUN1 retrograde signal antagonizes the light signalling pathway and converge on *GLK1* (Martín *et al.*, 2016). We show here that GUN1 controls the expression of *PIFs* (*PIF1*, 4, 5), *BZR1* and *BES1*, and *GLK1* in etiolated seedlings (Fig. 2a,b; Fig. 6; Fig. 7). At the critical stage of the initial light induced transcriptional activation, GUN1 is still present, repressing several *PIFs* (*PIF1*, 3, 4, and 8), *BRZ1*, *BES1*, and *GLK1*, and promoting *HY5* expression (Fig. 2a,b; Fig. 6; Fig. 7; Fig. S10). As chloroplast development progresses and the potential risk of oxidative damage decreases, GUN1 is degraded and is shown to reach a minimum at 24h when the chloroplasts are functional (Wu *et al.*, 2018). The reduced GUN1 levels lifts the negative plastid regulation of nuclear expression and allows for full expression of the *PhANGs* (Fig. 8).

Despite the large effect on gene expression, the *gun1* mutants do not demonstrate a constitutive photomorphogenic phenotype in the dark, similar to the well characterized *cop* and *det* mutants (Wei & Deng, 1996). In addition to the massive transcriptional changes, the transition from dark to light also results in a global increase in translational activity, with an altered translation of ~1/3 of all transcripts (Liu *et al.*, 2012). Moreover, reduced translation in the dark of specific photomorphogenic mRNAs has been linked to processing bodies (P-bodies), that regulate decay or translational arrest of the specific mRNAs (Jang *et al.*, 2019). Many components of the repressive network and their downstream genes controlled by GUN1 are under strict post-transcriptional regulation in the dark (Hernández-Verdeja *et al.*, 2020) and the increased expression observed in *gun1* may not correlate with an increase in the proteins required to enter photomorphogenesis. Thus, translational activity appears to be regulated by light-controlled mechanisms that are, to a

large extent, independent of GUN1. However, our proposed model for GUN1 could account for the subtle phenotype of *gun1* mutants, with higher Pchl_a accumulation in etiolated seedlings and lower survival rates when etiolated seedlings are exposed to light (Fig. S13) (Susek *et al.*, 1993; Xu *et al.*, 2016; Shimizu *et al.*, 2019). Our model could explain the second plastid dependent increase of nuclear transcription required for the final establishment of photosynthesis (Dubreuil *et al.*, 2018; Armarego-Marriott *et al.*, 2019) and once chloroplast development has reached a critical point, GUN1 is degraded (Fig. 2; Fig. S5; Fig. S6) and transcription of the *PhANGs* is boosted to achieve fully functional chloroplasts.

By using artificial stress conditions such as norflurazon and lincomycin, GUN1 has been assigned a role in communicating stress conditions in the plastids to the nucleus. Our results support that GUN1 relays the lincomycin-dependent retrograde signal also in the dark, and that this signal represses *PhANG* expression mainly through *GLK1* that is common to all transcriptomics profiles (Fig. 5; Fig. S8; Fig. S12). However, the small overlaps between the transcriptomics data suggest that GUN1 and lincomycin independently regulate specific gene sets. Although the experimental conditions for the transcriptomics analysis that were compared are somewhat different, three different available data sets for lincomycin treated seedlings provided similar results for the overlap between GUN1 in dark and following growth on lincomycin, which support the hypothesis of convergent and divergent signalling pathways for GUN1 and lincomycin. Our data strongly indicates that the inhibitors traditionally used to study retrograde signals lock the seedlings in the developmental state prevailing in darkness by stabilizing GUN1, and repressing *PhANGs*. This is supported by recent reports indicating that GUN1 is important to maintain Nuclear Encoded Polymerase activity for the transcriptional adaptive response (Δrpo phenotype) upon plastid impairment, promoting the transcriptional activity that prevails in non-developed plastids (Loudya *et al.*, 2020; Tadini *et al.*, 2020a). Any interference with plastid development, such as the conditions used in the mutant screen where *gun1* was identified (Susek *et al.*, 1993), will inhibit GUN1 degradation (Fig. 5; Fig. S8) (Wu *et al.*, 2018), nuclear gene expression will remain repressed and chloroplast development will not proceed (Dubreuil *et al.*, 2018).

Our data from the roots revealed a novel feature of GUN1 that could further support the role of GUN1 in maintaining non-photosynthetic plastid types. Plastids in the roots develop into colourless non-photosynthetic forms, generally termed leucoplasts and GUN1 was found in the

leucoplasts at high levels irrespective of light conditions (Fig. 2c,d; Fig. S5c,d). These results indicate that GUN1 degradation is dependent on normal progression of plastid-to-chloroplast development. This opens the question on organ specific GUN1 function and the regulation of GUN1 degradation. Plastid retrograde signals have been shown to be active in roots and at least the signals originated in response to defects in plastid translation are mediated by GUN1 and have effects on root development (Sullivan & Gray, 1999; Garnik *et al.*, 2019; Li *et al.*, 2020).

We demonstrate here that a true physiological function of GUN1 is to suppress expression of *PhANGs* in the dark and to protect the seedling during emergence from the soil by fine-tuning nuclear gene expression. Furthermore, the sustained accumulation of the GUN1 protein in the root tissue suggests that the regulatory mechanism behind the dynamics of GUN1 levels is only present in tissues that are normally exposed to light and have photosynthetic activity. Thus, not only does GUN1 act as a safeguard during the critical step of seedling emergence from darkness, GUN1 could also contribute to the organ-specific control of *PhANG* expression and chloroplast development.

Acknowledgements

This work was supported by grants from the 2020-03958, Swedish research foundation, (VR) and ARC19-0051, Foundation for Strategic Research (SSF) (ÅS). The authors would like to thank the UPSC Bioinformatics Facility for support with the data handling and computing.

Author contributions

T.H-V, L.V. and Å.S conceptualized the research, analysed data and wrote the paper. T.H-V, L.V., X.J., A.V., and C.D. performed the experiments. All authors read and approved the final version of the manuscript.

Data availability

Sequencing data and a description of samples are available at the European Nucleotide Archive (ENA) as accession PRJEB47885.

References

Alabadí D, Gallego-Bartolomé J, Orlando L, García-Cárcel L, Rubio V, Martínez C,

- Grigerio M, Iglesias-Pedraz JM, Espinosa A, Deng XW, et al. 2008.** Gibberellins modulate light signaling pathways to prevent Arabidopsis seedling de-etiolation in darkness. *The Plant Journal* **53**: 324–335.
- Armarego-Marriott T, Kowalewska LM, Burgos A, Fischer A, Thiele W, Erban A, Strand DD, Kahlau S, Hertle A, Kopka J, et al. 2019.** Highly resolved systems biology to dissect the etioplast-to-chloroplast transition in tobacco leaves. *Plant Physiology* **180**: 654–681.
- Armarego-Marriott T, Sandoval-ibañez O, Kowalewska L. 2020.** Beyond the darkness : recent lessons from etiolation and de-etiolation studies. *Journal of Experimental Botany* **71**: 1215–1225.
- Castillo-Davis CI, Hartl DL. 2003.** GeneMerge - Post-genomic analysis, data mining, and hypothesis testing. *Bioinformatics* **19**: 891–892.
- Cheminant S, Wild M, Bouvier F, Pelletier S, Renou J, Erhardt M, Hayes S, Terry MJ, Genschik P, Achard P. 2011.** DELLAs Regulate Chlorophyll and Carotenoid Biosynthesis to Prevent Photooxidative Damage during Seedling Deetiolation in Arabidopsis. *The Plant Cell* **23**: 1849–1860.
- Chen Y, Chen Y, Shi C, Huang Z, Zhang Y, Li S, Li Y, Ye J, Yu C, Li Z, et al. 2018.** SOAPnuke: A MapReduce acceleration-supported software for integrated quality control and preprocessing of high-throughput sequencing data. *GigaScience* **7**: 1–6.
- Clough SJ, Bent AF. 1998.** Floral dip: A simplified method for Agrobacterium-mediated transformation of *Arabidopsis thaliana*. *The Plant Journal* **16**: 735–743.
- Cottage A, Mott EK, Kempster JA, Gray JC. 2010.** The Arabidopsis plastid-signalling mutant *gun1* (genomes uncoupled1) shows altered sensitivity to sucrose and abscisic acid and alterations in early seedling development. *Journal of Experimental Botany* **61**: 3773–3786.
- Curtis MD, Grossniklaus U. 2003.** A Gateway Cloning Vector Set for High-Throughput Functional Analysis of Genes in Planta. *Plant Physiology* **133**: 462–469.
- Dietzel L, Gläßer C, Liebers M, Hiekel S, Courtois F, Czarnecki O, Schlicke H, Zubo Y, Börner T, Mayer K, et al. 2015.** Identification of Early Nuclear Target Genes of Plastidial Redox Signals that Trigger the Long-Term Response of Arabidopsis to Light Quality Shifts. *Molecular Plant* **8**: 1237–1252.
- Dong CJ, Liu JY. 2010.** The Arabidopsis EAR-motif-containing protein RAP2.1 functions as an active transcriptional repressor to keep stress responses under tight control. *BMC Plant Biology* **10**: 1–15.
- Dubreuil C, Jin X, de Dios Barajas-López J, Hewitt TC, Dobrenel T, Schröder WP, Hanson**

- J, Pesquet E, Grönlund A, Small I, et al. 2018.** Establishment of photosynthesis through chloroplast development is controlled by two distinct regulatory phases. *Plant Physiology* **176**: 1199–1214.
- Fristedt R, Williams-Carrier R, Merchant SS, Barkan A. 2014.** A thylakoid membrane protein harboring a DnaJ-type zinc finger domain is required for photosystem I accumulation in plants. *Journal of Biological Chemistry* **289**: 30657–30667.
- Garnik EY, Tarasenko VI, Gorbunova AI, Shmakov VN, Konstantinov YM. 2019.** Genome uncoupled (gun) phenotype is associated with root growth repression in Arabidopsis seedlings grown on lincomycin. *Theoretical and Experimental Plant Physiology* **31**: 445–454.
- Hernández-Verdeja T, Strand Å. 2018.** Retrograde signals navigate the path to chloroplast development. *Plant Physiology* **176**: 967–976.
- Hernández-Verdeja T, Vuorijoki L, Strand Å. 2020.** Emerging from the darkness: interplay between light and plastid signalling during chloroplast biogenesis. *Physiologia Plantarum* **169**: 397–406.
- Hills AC, Khan S, López-Juez E. 2015.** Chloroplast biogenesis-associated nuclear genes: control by plastid signals evolved prior to their regulation as part of photomorphogenesis. *Frontiers in Plant Science* **6**: 1078.
- Hooper CM, Castleden IR, Tanz SK, Aryamanesh N, Millar AH. 2017.** SUBA4: The interactive data analysis centre for Arabidopsis subcellular protein locations. *Nucleic Acids Research* **45**: D1064–D1074.
- Jiao Y, Lau OS, Deng XW. 2007.** Light-regulated transcriptional networks in higher plants. *Nature Reviews Genetics* **8**: 207–230.
- Jiao Y, Ma L, Strickland E, Deng XW. 2005.** Conservation and divergence of light-regulated genome expression patterns during seedling development in rice and Arabidopsis. *The Plant Cell* **17**: 3239–3256.
- Jin J, Zhang H, Kong L, Gao G, Luo J. 2014.** PlantTFDB 3.0: A portal for the functional and evolutionary study of plant transcription factors. *Nucleic Acids Research* **42**: 1182–1187.
- Kakizaki T, Matsumura H, Nakayama K, Che FSF-S, Terauchi R, Inaba T, Oa RSW, Kakizaki T, Matsumura H, Nakayama K, et al. 2009.** Coordination of Plastid Protein Import and Nuclear Gene Expression by Plastid-to-Nucleus Retrograde Signaling. *Plant Physiology* **151**: 1339–1353.
- Kindgren P, Kremnev D, Blanco NE, de Dios Barajas López J, Fernández AP, Tellgren-Roth**

- C, Small I, Strand Å. 2012a.** The *plastid redox insensitive 2* mutant of Arabidopsis is impaired in PEP activity and high light-dependent plastid redox signalling to the nucleus. *The Plant Journal* **70**: 279–291.
- Kindgren P, Norén L, Barajas López JDD, Shaikhali J, Strand Å. 2012b.** Interplay between HEAT SHOCK PROTEIN 90 and HY5 controls PhANG expression in response to the GUN5 plastid signal. *Molecular Plant* **5**: 901–913.
- Koussevitzky S, Nott A, Mockler TC, Hong F, Sachetto-Martins G, Surpin M, Lim J, Mittler R, Chory J. 2007.** Signals from Chloroplasts Converge to Regulate Nuclear Gene Expression. *Science (New York, N.Y.)* **316**: 715–719.
- Kulkarni SR, Vaneechoutte D, Velde J Van De, Vandepoele K. 2018.** TF2Network : predicting transcription factor regulators and gene regulatory networks in Arabidopsis using publicly available binding site information. *Nucleic Acids Research* **46**: e31.
- Langmead B, Salzberg SL. 2012.** Fast gapped-read alignment with Bowtie 2. *Nature Methods* **9**: 357–359.
- Leivar P, Monte E. 2014.** PIFs: systems integrators in plant development. *The Plant Cell* **26**: 56–78.
- Li B, Dewey CN. 2011.** RSEM: accurate transcript quantification from RNA-seq data with or without a reference genome. *BMC Bioinformatics* **12**: 323.
- Li P, Ma J, Sun X, Zhao C, Ma C, Wang X. 2020.** RAB GTPASE HOMOLOG 8D is required for maintenance of both the root stem cell niche and meristem. *The Plant Journal* **105**: 1225-1239.
- Liu Y, Li X, Ma D, Chen Z, Wang J, Liu H. 2018.** CIB1 and CO interact to mediate CRY2-dependent regulation of flowering. *EMBO Reports* **19**: 1–10.
- Liu X, Liu R, Li Y, Shen X, Zhong S, Shi H. 2017.** EIN3 and PIF3 Form an Interdependent Module that Represses Chloroplast Development in Buried Seedlings. *The Plant Cell* **29**: 3051–3067.
- Llamas E, Pulido P, Rodriguez-Concepcion M. 2017.** Interference with plastome gene expression and Clp protease activity in Arabidopsis triggers a chloroplast unfolded protein response to restore protein homeostasis. *PLoS Genetics* **13**: 1–27.
- Loudya N, Okunola T, He J, Jarvis P, López-juez E. 2020.** Retrograde signalling in a virescent mutant triggers an anterograde delay of chloroplast biogenesis that requires GUN1 and is essential for survival. *Philosophical Transactions of the Royal Society, B* **375**: 20190400.
- Love MI, Huber W, Anders S. 2014.** Moderated estimation of fold change and dispersion for

RNA-seq data with DESeq2. *Genome Biology* **15**: 1–21.

Mangiafico S. 2019. rcompanion: Functions to Support Extension Education Program Evaluation. R package version 2.3.25. <https://CRAN.R-project.org/package=rcompanion>

Marino G, Naranjo B, Wang J, Penzler JF, Kleine T, Leister D. 2019. Relationship of GUN1 to FUG1 in chloroplast protein homeostasis. *The Plant Journal* **99**: 521–535.

Martín G, Leivar P, Ludevid D, Tepperman JM, Quail PH, Monte E. 2016. Phytochrome and retrograde signalling pathways converge to antagonistically regulate a light-induced transcriptional network. *Nature Communications* **7**: 11431.

Ni F, Wu L, Wang Q, Hong J, Qi Y, Zhou X. 2017. Turnip Yellow Mosaic Virus P69 Interacts with and Suppresses GLK Transcription Factors to Cause Pale-Green Symptoms in Arabidopsis. *Molecular Plant* **10**: 764–766.

Norén L, Kindgren P, Stachula P, Rühl M, Eriksson ME, Hurry V, Strand Å. 2016. Circadian and plastid signaling pathways are integrated to ensure correct expression of the CBF and COR genes during photoperiodic growth. *Plant Physiology* **171**: 1392–1406.

Ogle DH, Wheeler P, Dinno A. 2019. FSA: Fisheries Stock Analysis. R package version 0.8.30, <https://github.com/droglenc/FSA>.

Oh E, Zhu J-Y, Wang Z-Y. 2012. Interaction between BZR1 and PIF4 integrates brassinosteroid and environmental responses. *Nature Cell Biology* **14**: 802–809.

Oliveros JC. 2015. Venny. An interactive tool for comparing lists with Venn's diagrams. *Venny. An interactive tool for comparing lists with Venn's diagrams.* <https://bioinfogp.cnb.csic.es/tools/venny/index.html>

op den Camp RG., Przybyla D, Ochsenbein C, Laloi C, Kim C, Danon A, Wagner D, Hideg É, Göbel C, Feussner I, et al. 2013. Rapid Induction of Distinct Stress Responses after the Release of Singlet Oxygen in Arabidopsis. *The Plant Cell* **15**: 2320–2332.

Peng H, Zhao J, Neff MM. 2015. ATAF2 integrates arabidopsis brassinosteroid inactivation and seedling photomorphogenesis. *Development (Cambridge)* **142**: 4129–4138.

Pesquet E, Korolev A V, Calder G, Lloyd CW, Centre JI, Lane C. 2010. The Microtubule-Associated Protein AtMAP70-5 Regulates Secondary Wall Patterning in Arabidopsis Wood Cells. *Current Biology* **20**: 744–749.

Pham VN, Kathare PK, Huq E. 2018. Phytochromes and Phytochrome Interacting Factors. *Plant Physiology* **176**: pp.01384.2017.

Pogson BJ, Ganguly D, Albrecht-Borth V. 2015. Insights into chloroplast biogenesis and

development. *Biochimica et Biophysica Acta (BBA) - Bioenergetics* **1847**: 1016–1024.

R Core Team. 2019. R: A language and environment for statistical computing. R Foundation for Statistical Computing, Vienna, Austria. <https://www.R-project.org/>

Ramakers C, Ruijter JM, Lekanne Deprez RH, Moorman AFM. 2003. Assumption-free analysis of quantitative real-time polymerase chain reaction (PCR) data. *Neuroscience Letters* **339**: 62–66.

Richter AS, Tohge T, Fernie AR, Grimm B. 2020. The genomes uncoupled -dependent signalling pathway coordinates plastid biogenesis with the synthesis of anthocyanins. *Philosophical Transactions of the Royal Society, B* **375**: 20190403.

RStudio Team. 2016. RStudio: Integrated Development for R. RStudio, Inc., Boston, MA <http://www.rstudio.com/>

Ruckle ME, Larkin RM. 2009. Plastid signals that affect photomorphogenesis in *Arabidopsis thaliana* are dependent on GENOMES UNCOUPLED 1 and cryptochrome 1. *New Phytologist* **182**: 367–379.

Schindelin J, Arganda-Carreras I, Frise E, Kaynig V, Longair M, Pietzsch T, Preibisch S, Rueden C, Saalfeld S, Schmid B, et al. 2012. Fiji: An open-source platform for biological-image analysis. *Nature Methods* **9**: 676–682.

Schneider A, Steinberger I, Strissel H, Kunz HH, Manavski N, Meurer J, Burkhard G, Jarzombski S, Schünemann D, Geimer S, et al. 2014. The Arabidopsis Tellurite resistance C protein together with ALB3 is involved in photosystem II protein synthesis. *The Plant Journal* **78**: 344–356.

Seluzicki A, Burko Y, Chory J. 2017. Dancing in the dark: darkness as a signal in plants. *Plant Cell and Environment Cell Environ* **40**: 2487–2501.

Shaikhali J, Norén L, De Dios Barajas-López J, Srivastava V, König J, Sauer UH, Wingsle G, Dietz KJ, Strand Å. 2012. Redox-mediated mechanisms regulate DNA binding activity of the G-group of basic region leucine zipper (bZIP) transcription factors in Arabidopsis. *Journal of Biological Chemistry* **287**: 27510–27525.

Shannon P, Markiel A, Ozier O, Baliga NS, Wang JT, Ramage D, Amin N, Schwikowski B, Ideker T. 2003. Cytoscape: A software environment for integrated models of biomolecular interaction networks. *Genome Research* **13**: 2498–2504.

Shimizu T, Kacprzak SM, Mochizuki N, Nagatani A, Watanabe S, Shimada T, Tanaka K, Hayashi Y, Arai M, Leister D, et al. 2019. The retrograde signaling protein GUN1 regulates

tetrapyrrole biosynthesis. *Proceedings of the National Academy of Sciences of the United States of America* **116**: 24900–24906.

Sullivan J, Gray J. 1999. Plastid translation is required for the expression of nuclear photosynthesis genes in the dark and in roots of the pea *lip1* mutant. *The Plant Cell* **11**: 901–10.

Sun X, Feng P, Xu X, Guo H, Ma J, Chi W, Lin R, Lu C, Zhang L. 2011. A chloroplast envelope-bound PHD transcription factor mediates chloroplast signals to the nucleus. *Nature Communications* **2**: 477.

Supek F, Bošnjak M, Škunca N, Šmuc T. 2011. Revigo summarizes and visualizes long lists of gene ontology terms. *PLoS ONE* **6**: e21800.

Susek RE, Ausubel FM, Chory J. 1993. Signal-Transduction Mutants of Arabidopsis Uncouple Nuclear Cab and RbcS Gene-Expression from Chloroplast Development. *Cell* **74**: 787–799.

Tadini L, Jeran N, Peracchio C, Masiero S, Colombo M, Pesaresi P. 2020a. The plastid transcription machinery and its coordination with the expression of nuclear genome: Plastid-Encoded Polymerase, Nuclear-Encoded Polymerase and the Genomes Uncoupled 1-mediated retrograde communication. *Philosophical Transactions of the Royal Society, B* **375**: 20190399.

Tadini L, Peracchio C, Trotta A, Colombo M, Mancini I, Jeran N, Costa A, Faoro F, Marsoni M, Vannini C, et al. 2020b. GUN1 influences the accumulation of NEP-dependent transcripts and chloroplast protein import in Arabidopsis cotyledons upon perturbation of chloroplast protein homeostasis. *The Plant Journal* **101**: 1198–1220.

Tadini L, Pesaresi P, Kleine T, Rossi F, Guljamow A, Sommer F, Mühlhaus T, Schroda M, Masiero S, Pribil M, et al. 2016. GUN1 controls accumulation of the Plastid Ribosomal Protein S1 at the protein level and interacts with proteins involved in plastid protein homeostasis. *Plant Physiology* **170**: 1817–1830.

Tamai H, Iwabuchi M, Meshi T. 2002. Arabidopsis GARP transcriptional activators interact with the Pro-rich activation domain shared by G-box-binding bZIP factors. *Plant and Cell Physiology* **43**: 99–107.

Terasawa K, Sato N. 2005. Visualization of plastid nucleoids in situ using the PEND-GFP fusion protein. *Plant and Cell Physiology* **46**: 649–660.

Tokumar M, Adachi F, Toda M, Ito-Inaba Y, Yazu F, Hirosawa Y, Sakakibara Y, Suiko M, Kakizaki T, Inaba T. 2017. Ubiquitin-proteasome dependent regulation of the GOLDEN2-LIKE 1 transcription factor in response to plastid signals. *Plant Physiology* **173**: 524–535.

Waters MT, Wang P, Korkaric M, Capper RG, Saunders NJ, Langdale JA. 2009. GLK

Transcription Factors Coordinate Expression of the Photosynthetic Apparatus in Arabidopsis. *The Plant Cell* **21**: 1109–1128.

Wei N, Deng XW. 1996. The role of the COP/DET/FUS genes in light control of arabidopsis seedling development. *Plant Physiology* **112**: 871–878.

Wickham H. 2016. *ggplot2: Elegant Graphics for Data Analysis*. Springer-Verlag New York.

Woodson JD, Perez-Perez J, Schmitz RJ, Ecker JR, Chory J. 2013. Sigma factor-mediated plastid retrograde signals control nuclear gene expression. *The Plant Journal* **73**: 1–13.

Woodson JD, Perez-Ruiz JM, Chory J. 2011. Heme synthesis by plastid ferrochelatase 1 regulates nuclear gene expression in plants. *Current Biology* **21**: 897–903.

Wu G-Z, Chalvin C, Hoelscher MP, Meyer EH, Wu XN, Bock R. 2018. Control of Retrograde Signaling by Rapid Turnover of GENOMES UNCOUPLED 1. *Plant Physiology* **176**: 2472–2495.

Wu G-Z, Meyer EH, Richter AS, Schuster M, Ling Q, Schöttler MA, Walther D, Zoschke R, Grimm B, Jarvis RP, et al. 2019a. Control of retrograde signalling by protein import and cytosolic folding stress. *Nature Plants* **5**: 525–538.

Wu G-Z, Meyer EH, Wu S, Bock R. 2019b. Extensive Posttranscriptional Regulation of Nuclear Gene Expression by Plastid Retrograde Signals. *Plant Physiology* **180**: 2034–2048.

Xu D. 2020. COP1 and BBXs-HY5-mediated light signal transduction in plants. *New Phytologist* **228**: 1748–1753.

Xu X, Chi W, Sun X, Feng P, Guo H, Li J, Lin R, Lu C, Wang H, Leister D, et al. 2016. Convergence of light and chloroplast signals for de-etiolation through ABI4–HY5 and COP1. *Nature Plants* **2**: 16066.

Yamaguchi M, Kubo M, Fukuda H, Demura T. 2008. Vascular-related NAC-DOMAIN7 is involved in the differentiation of all types of xylem vessels in Arabidopsis roots and shoots. *The Plant Journal* **55**: 652–664.

Yang EJ, Yoo CY, Liu J, Wang H, Cao J, Li F-W, Pryer KM, Sun T, Weigel D, Zhou P, et al. 2019. NCP activates chloroplast transcription by controlling phytochrome-dependent dual nuclear and plastidial switches. *Nature Communications* **10**: 2630.

Yoo CY, Pasoreck EK, Wang H, Cao J, Blaha GM, Weigel D, Chen M. 2019. Phytochrome activates the plastid-encoded RNA polymerase for chloroplast biogenesis via nucleus-to-plastid signaling. *Nature Communications* **10**: 2629.

Yu X, Li L, Zola J, Aluru M, Ye H, Foudree A, Guo H, Anderson S, Aluru S, Liu P, et al. 2011. A brassinosteroid transcriptional network revealed by genome-wide identification of BESI

target genes in *Arabidopsis thaliana*. *The Plant Journal* **65**: 634–646.

Zhao X, Huang J, Chory J. 2019. GUN1 interacts with MORF2 to regulate plastid RNA editing during retrograde signaling. *Proceedings of the National Academy of Sciences of the United States of America* **116**: 10162–10167.

Zhong S, Zhao M, Shi T, Shi H, An F, Zhao Q, Guo H. 2009. EIN3/EIL1 cooperate with PIF1 to prevent photo-oxidation and to promote greening of *Arabidopsis* seedlings. *Proceedings of the National Academy of Sciences of the United States of America* **106**: 21431–21436.

Figure legends

Fig. 1. GUN1:YFP and *GUN1* silencing in *Arabidopsis* cell culture. (a) Representative images of GUN1:YFP fluorescence in 7d-old dark grown (0d) and 1d and 5d of constant white light ($150 \mu\text{mol photons m}^{-2} \text{s}^{-1}$) exposed *GUN1:YFP #24 PEND #5* *Arabidopsis* cells transformed with *P_{GUN1}:GUN1:YFP* construct. PEND:CFP was used as a marker for plastids. All the images were taken using the same confocal microscope settings. Bar = $10 \mu\text{m}$. (b) *LHCB1.1* and *LHCB2.4* log₂ relative expression in *amiGUN1 #4* transgenic cells treated with ethanol (mock) or β -estradiol (β -Est) to silence *GUN1* and grown in dark for 5 days (D 5d) and 1 or 5 days (L 1d, L5d) following constant light exposure ($150 \mu\text{mol photons m}^{-2} \text{s}^{-1}$). Gene expression was normalized to *ATIG13320* and calibrated to 1 relative to mock treated cells D 5d. Data represents the mean \pm SE of the mean. Significance of the differences were determined by Wilcoxon test, $p < 0.001$ ***.

Fig. 2. GUN1:YFP in dark-grown and light-exposed *Arabidopsis* seedlings. (a) Fluorescence of GUN1:YFP in 5d-old etiolated cotyledons of *gun1-102 GUN1:YFP #6.1.1* seedlings exposed 0, 1, 6 or 24h to constant light ($150 \mu\text{mol photons m}^{-2} \text{s}^{-1}$). Bar = $100 \mu\text{m}$. (b) Quantification of GUN1:YFP based on fluorescence intensity (arbitrary units; a.u.) in plastids of seedlings grown as in (a). Results from three independent replicates, with 4 or 5 cotyledons per replicate and time point, and 20 chloroplasts per cotyledon (total n in brackets). (c) Fluorescence of GUN1:YFP in 5d-old etiolated roots of *gun1-102 GUN1:YFP #6.1.1* seedlings exposed 0 or 24h to constant light ($150 \mu\text{mol photons m}^{-2} \text{s}^{-1}$). Bar = $20 \mu\text{m}$. (d) Quantification of GUN1:YFP based on fluorescence intensity (arbitrary units; a.u.) in plastids of roots grown as in (c). Results from 3 or 5 roots and 15 chloroplasts per root (total n in brackets). (a,c) All the images were taken using the same confocal microscopy settings. (b,d) Box-plot center lines show the medians and plus show the mean of all the fluorescence intensity measurements; box limits indicate the 25th and 75th percentiles;

whiskers extend 1.5 times the interquartile range from the 25th and 75th percentiles; potential outliers are plotted as circles. Significance of the differences and differences between groups were determined with a Kruskal-Wallis test, (b) $p < 2.2e^{-16}$ and (d) $p < 1.7e^{-7}$, and a post-hoc Dunn's test with Bonferroni correction. Groups sharing a letter do not differ significantly ($\alpha = 0.05$).

Fig. 3. Transcriptomic analysis of dark-grown and light-exposed WT and *gun1-102* Arabidopsis seedlings. (a) Number of differentially expressed genes (DEGs) in the *gun1-102* seedlings compared to the WT. Up- and down-regulated genes are shown for etiolated (D 0h), and de-etiolated for 3 (L 3h) or 24h (L 24h). (b) Venn diagrams showing the overlaps between conditions for the up- and down-regulated genes in *gun1-102*. The DEGs exclusively deregulated in dark, dark and light or only in light are highlighted in grey, yellow or green, respectively. (c) Relative subcellular localization of the protein products in *gun1-102* DEGs. Estimation of the subcellular abundance was done with SUBcellular location database of Arabidopsis proteins (SUBA4) based on published experimental data sets. Standard represents all available TAIR10 AGIs with assigned high confidence subcellular localization.

Fig. 4. Gene ontology (GO) enrichment analysis of deregulated genes in *gun1-102*. (a) Selected GO terms enriched in up-regulated genes in etiolated (D 0h) and de-etiolated (L 3h) *gun1-102* Arabidopsis seedlings. (b) Selected GO terms enriched in down-regulated genes in etiolated (D 0h) and de-etiolated (L 3h) *gun1-102* seedlings. (a,b) The size of the circles indicates the percentage of the deregulated genes, and the colour intensity indicates the significance (p-value Bonferroni correction). The complete tables of enriched GO terms are in Supporting Information Fig. S5.

Fig. 5. GUN1:YFP response to lincomycin and comparison of etiolated *gun1-102* differentially expressed genes (DEGs) with *gun1* or WT Arabidopsis seedlings treated with lincomycin. (a) Fluorescence of GUN1:YFP in 5d-old etiolated cotyledons of *gun1-103 GUN1:YFP #6.3.6* seedlings grown with or without lincomycin and exposed 0 or 24h to light. Bar = 100 μm . (b) Quantification of GUN1:YFP based on fluorescence intensity (arbitrary units; a.u.) in plastids seedlings grown as in (a). Results from three independent replicates, with 3 cotyledons per replicate and time point, and 15 chloroplasts per cotyledon (total n in brackets). Box-plot center lines show the medians and plus show the mean of all the fluorescence intensity measurements;

box limits indicate the 25th and 75th percentiles; whiskers extend 1.5 times the interquartile range from the 25th and 75th percentiles; potential outliers are plotted as circles. Significance of the differences and differences between groups were determined with a Kruskal-Wallis test, $p < 2.2 \times 10^{-16}$, and a post-hoc Dunn's test with Bonferroni correction. Groups sharing a letter do not differ significantly ($\alpha = 0.05$). (c) Venn diagrams show the overlaps between *gun1-102* up-regulated DEGs in etiolated seedlings (D 0h Up) and *gun1* up-regulated DEGs in seedlings grown with lincomycin in light (Lin L Up) or WT down-regulated DEGs in seedlings grown with lincomycin in light (Lin L Down) or dark (Lin D Down).

Fig. 6. Up-regulated transcription factors in Arabidopsis *gun1-102*. Heatmap of the 92 up-regulated transcription factors in *gun1-102* with potential targets among the differentially expressed genes (DEGs) according to TF2Network. FC, fold change.

Fig. 7. Gene regulatory network (GRN) representation of predicted regulatory interactions of 92 up-regulated Arabidopsis transcription factors (TFs) and their respective differentially expressed genes (DEGs) targets are represented. Positive co-expression values and motifs overrepresented on promoters of target DEGs were considered to create regulatory interactions. Only the main connected component is represented. Sizes of TF nodes are proportional to the number of connections. A file with the network information is available in Supporting Information Table S7.

Fig. 8. Working model for GUN1 during chloroplast biogenesis in Arabidopsis. GUN1 is present in proplastids and etioplasts giving rise to a retrograde signal that regulates a large number of critical transcription factors (TFs) linked to light response, photomorphogenesis, and chloroplast development, and consequently their downstream genes. As the light response proceeds, GUN1 levels decrease through CLPC degradation, the regulation of TFs and their downstream genes is released, transcription of *PhANGs* is boosted and the establishment of fully functional chloroplasts is achieved. In the nucleus are depicted representative GUN1-repressed TFs only in etiolated seedlings (grey), in etiolated and de-etiolated seedlings (yellow), or only in de-etiolated seedlings (green). Sizes of TFs are relative to their amount of connections in the GRN (Fig. 7 and Supporting Information Table S7).

Supplementary information

Figure S1. Volcano plots showing the selection of significant DEGs.

Figure S2. GUN1:YFP and *GUN1* silencing in Arabidopsis cell culture.

Figure S3. Complementation analysis of *gun1* mutants with $P_{GUN1}:GUN1:YFP$.

Figure S4. GUN1:YFP fluorescence and gene expression in etiolated and de-etiolated *gun1 GUN1:YFP* seedlings.

Figure S5. GUN1:YFP in dark-grown and light-exposed *gun1-103 GUN1:YFP* #6.3.6 seedlings.

Figure S6. Immunoblot analysis of GUN1:YFP during the greening process.

Figure S7. Gene ontology enrichment analysis of deregulated genes in *gun1-102*.

Figure S8. GUN1:YFP response to lincomycin and comparison of de-etiolated *gun1-102* DEGs with *gun1* or WT seedlings treated with lincomycin.

Figure S9. Comparison of *gun1-102* up-regulated genes with GLK induced genes.

Figure S10. Functional analysis of deregulated transcription factors in *gun1-102*.

Figure S11. Expression levels from the RNA-seq replicates and qPCR validation for selected transcription factors.

Figure S12. Transcription factors involved in photomorphogenesis deregulated in *gun1-102* compared with lincomycin transcriptomic data.

Figure S13. Greening rate, survival and Pchl_a accumulation of etiolated *gun1* seedlings.

Methods S1. Protein extraction, electrophoresis and immunoblotting.

Table S1. Oligonucleotide sequences of primers used in this study.

Table S2. RNA-Seq reads filtering summary.

Table S3. Differential expressed genes with raw values of filter parameters.

Table S4. Gene Ontology enrichment analysis of DEGs.

Table S5. Gene Ontology enrichment analysis of common DEGs of *gun1-102* and lincomycin transcriptomic data.

Table S6. GLK targets in common DEGs of *gun1-102* and lincomycin transcriptomic data.

Table S7. GRN topology data and outgoing neighbours.

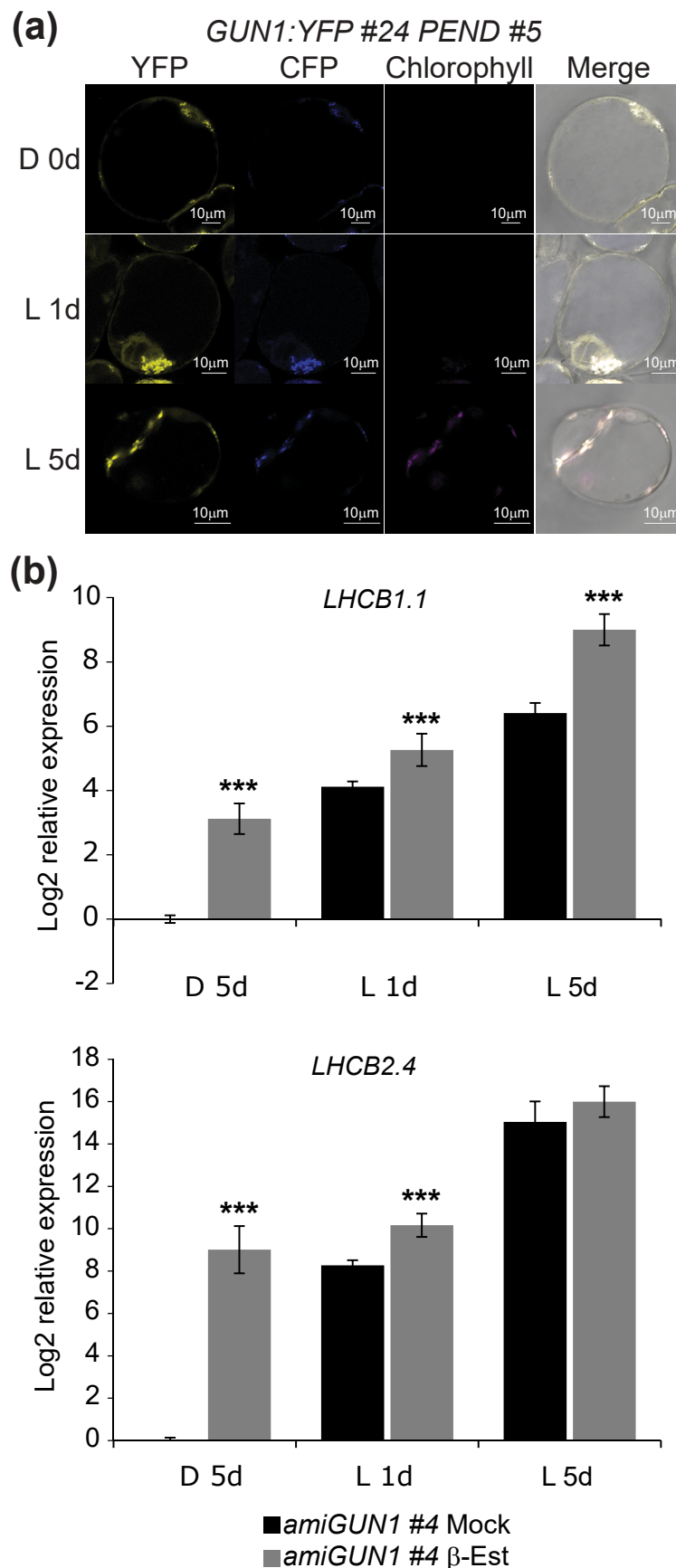


Fig. 1. *GUN1:YFP* and *GUN1* silencing in *Arabidopsis* cell culture. (a) Representative images of *GUN1:YFP* fluorescence in dark grown (D 0d) and 1d or 5d of constant white light ($150 \mu\text{mol photons m}^{-2} \text{s}^{-1}$) exposed *GUN1:YFP #24 PEND #5* *Arabidopsis* cells transformed with $P_{GUN1}:GUN1:YFP$ construct. *PEND:CFP* was used as a marker for plastids. All the images were taken using the same confocal microscope settings. Bar = $10 \mu\text{m}$. (b) *LHCB1.1* and *LHCB2.4* \log_2 relative expression in *amiGUN1 #4* transgenic cells treated with ethanol (mock) or β -estradiol (β -Est) to silence *GUN1* and grown in dark for 5 days (D 5d) and 1 or 5 days (L 1d, L 5d) following constant light exposure ($150 \mu\text{mol photons m}^{-2} \text{s}^{-1}$). Gene expression was normalized to *ATIG13320* and calibrated to 1 relative to mock treated cells D 5d. Data represents the mean \pm SE of the mean. Significance of the differences were determined by Wilcoxon test, $p < 0.001$ ***.

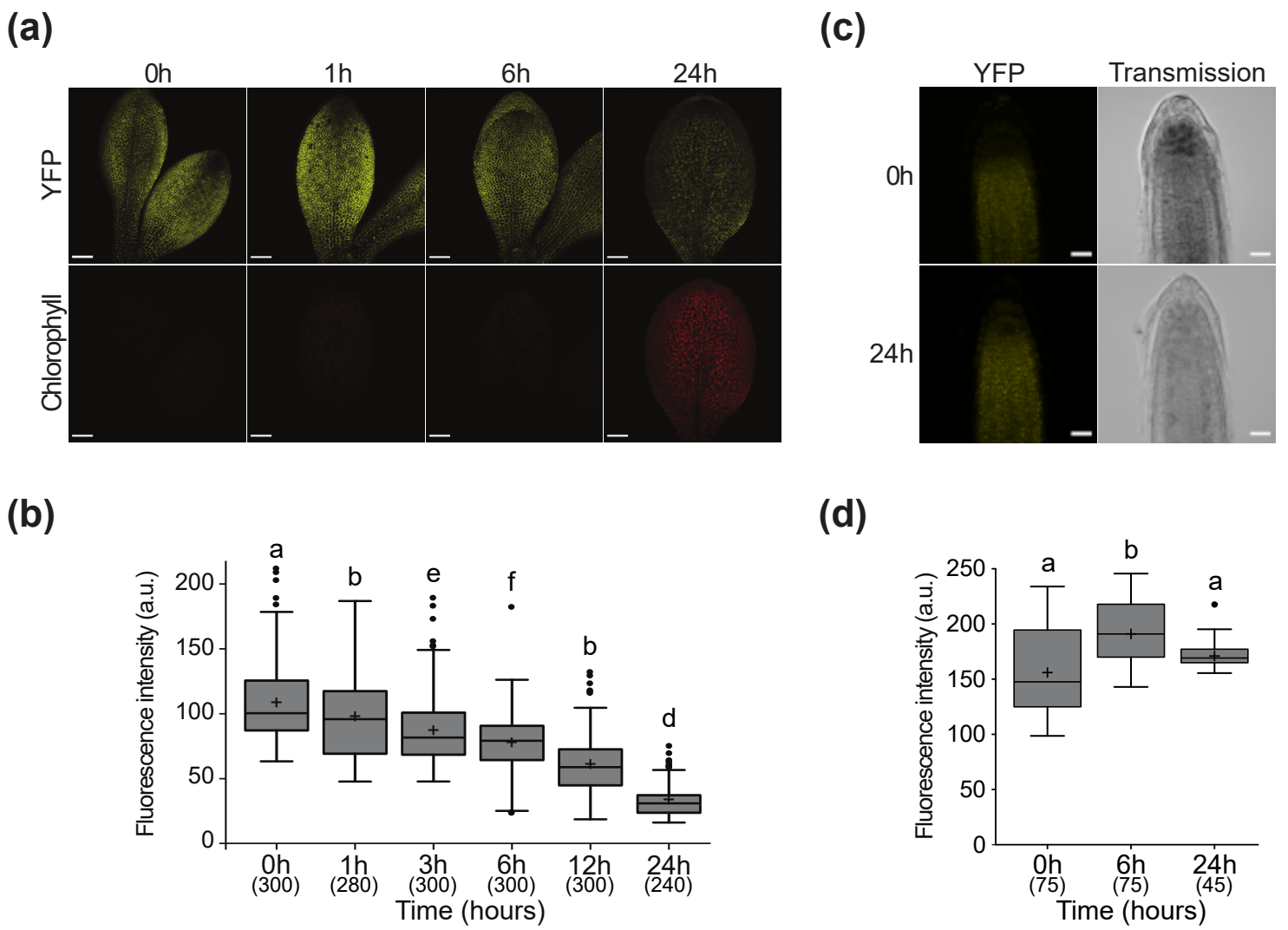


Fig. 2. GUN1:YFP in dark-grown and light-exposed *Arabidopsis* seedlings. (a) Fluorescence of GUN1:YFP in 5d-old etiolated cotyledons of *gun1-102 GUN1:YFP #6.1.1* seedlings exposed 0, 1, 6 or 24h to constant light ($150 \mu\text{mol photons m}^{-2} \text{s}^{-1}$). Bar = 100 μm . (b) Quantification of GUN1:YFP based on fluorescence intensity (arbitrary units; a.u.) in plastids of seedlings grown as in (a). Results from three independent replicates, with 4 or 5 cotyledons per replicate and time point, and 20 chloroplasts per cotyledon (total n in brackets). (c) Fluorescence of GUN1:YFP in 5d-old etiolated roots of *gun1-102 GUN1:YFP #6.1.1* seedlings exposed 0 or 24h to constant light ($150 \mu\text{mol photons m}^{-2} \text{s}^{-1}$). Bar = 20 μm . (d) Quantification of GUN1:YFP based on fluorescence intensity (arbitrary units; a.u.) in plastids of roots grown as in (c). Results from 3 or 5 roots and 15 chloroplasts per root (total n in brackets). (a,c) All the images were taken using the same confocal microscope settings. (b,d) Box-plot center lines show the medians and plus show the mean of all the fluorescence intensity measurements; box limits indicate the 25th and 75th percentiles; whiskers extend 1.5 times the interquartile range from the 25th and 75th percentiles; potential outliers are plotted as circles. Significance of the differences and differences between groups were determined with a Kruskal-Wallis test, (b) $p < 2.2e^{-16}$ and (d) $p < 1.7e^{-7}$, and a post-hoc Dunn's test with Bonferroni correction. Groups sharing a letter do not differ significantly ($\alpha = 0.05$).

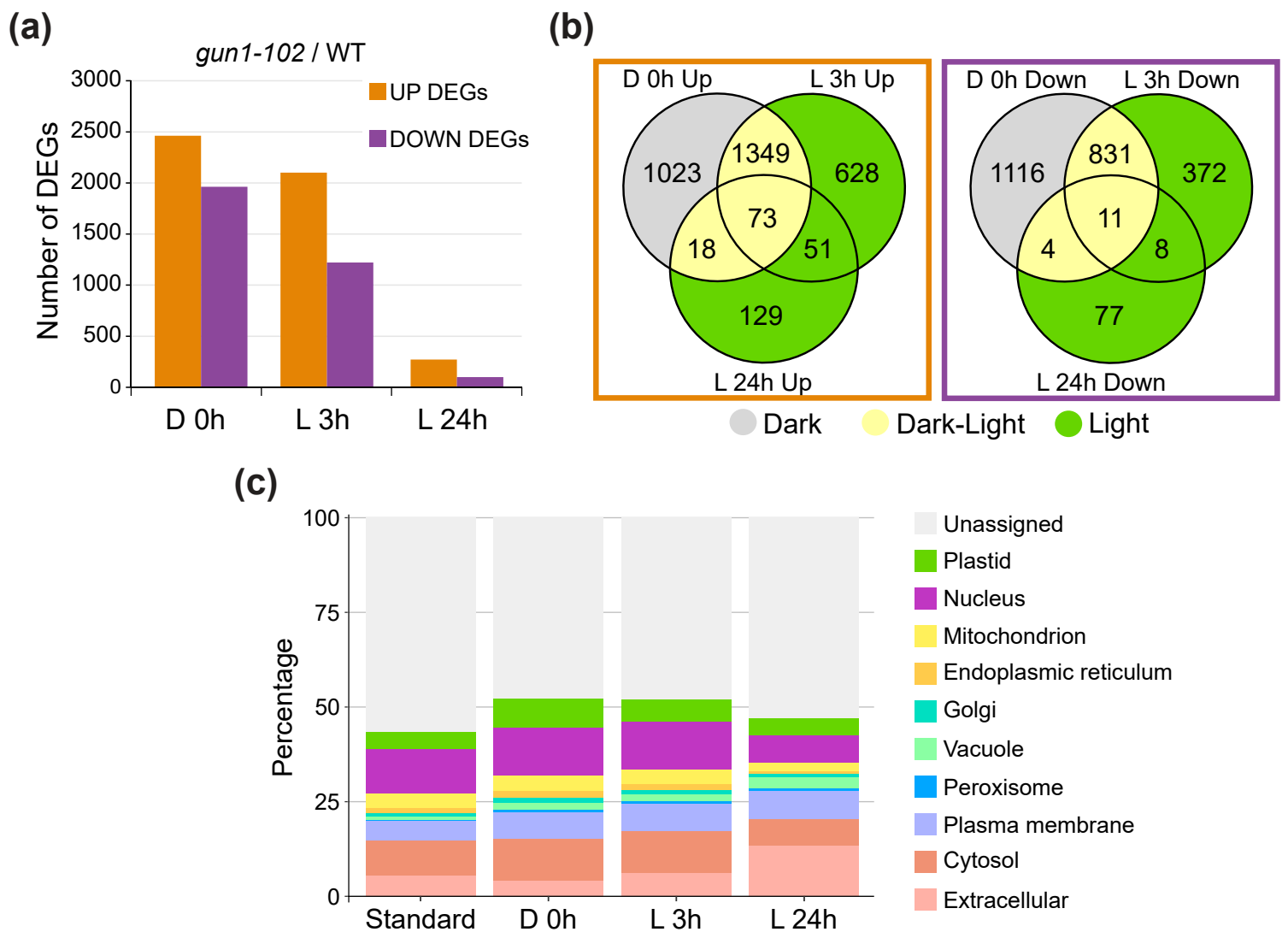


Fig. 3. Transcriptomic analysis of dark-grown and light-exposed WT and *gun1-102* Arabidopsis seedlings. (a) Number of differentially expressed genes (DEGs) in the *gun1-102* seedlings compared to the WT. Up- and down-regulated genes are shown for etiolated (D 0h), and de-etiolated for 3 (L 3h) or 24h (L 24h). (b) Venn diagrams showing the overlaps between conditions for the up- and down-regulated genes in *gun1-102*. The DEGs exclusively deregulated in dark, dark and light or only in light are highlighted in grey, yellow or green, respectively. (c) Relative subcellular localization of the protein products of *gun1-102* DEGs. Estimation of the subcellular abundance was done with SUBcellular location database of Arabidopsis proteins (SUBA4) based on published experimental data sets. Standard represents all available TAIR10 AGIs with assigned high confidence subcellular localization.

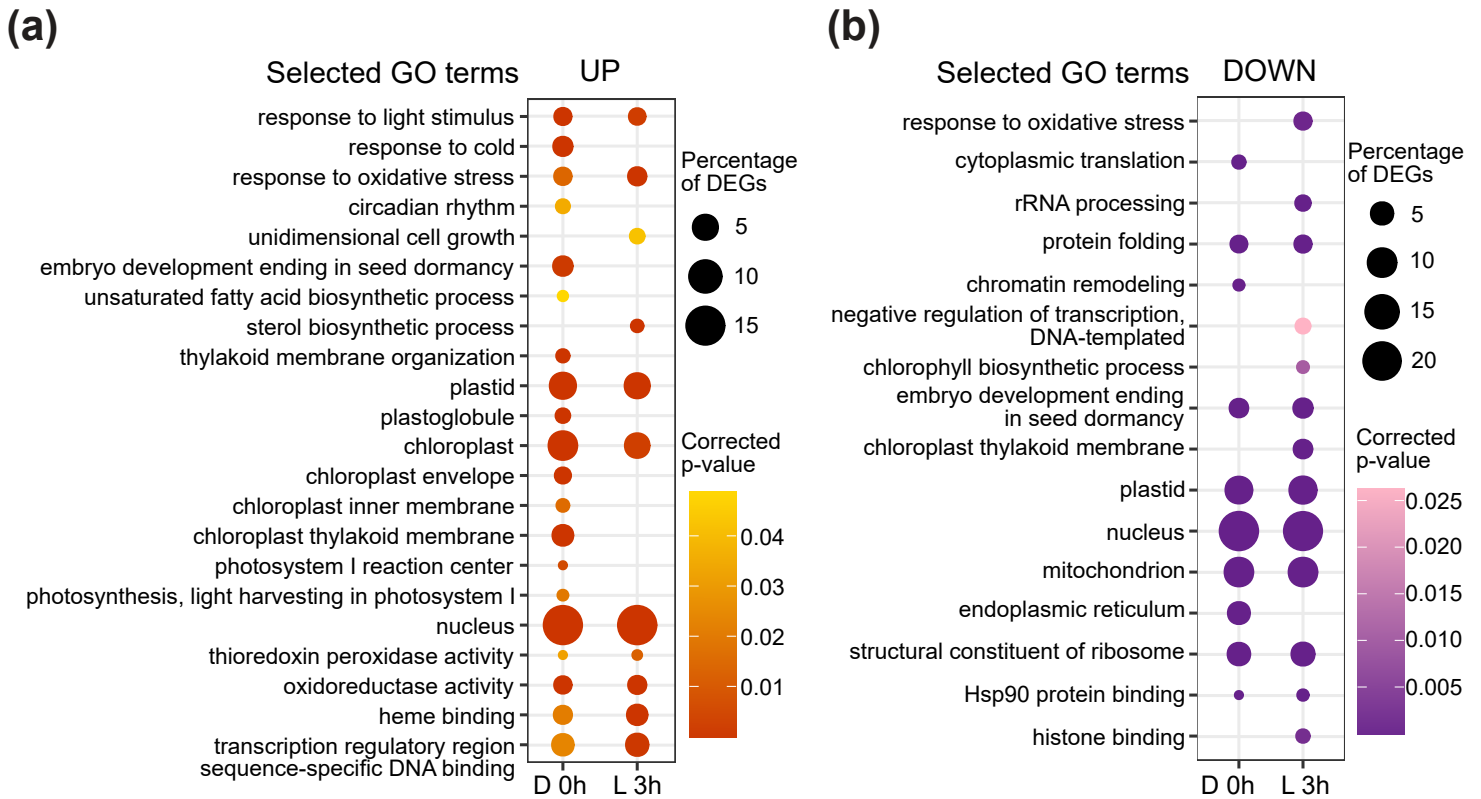


Fig. 4. Gene ontology enrichment analysis of deregulated genes in *gun1-102*. (a) Selected GO terms enriched in up-regulated genes in etiolated (D 0h) and de-etiolated (L 3h) *gun1-102* Arabidopsis seedlings. (b) Selected GO terms enriched in down-regulated genes in etiolated (D 0h) and de-etiolated (L 3h) *gun1-102* seedlings. (a,b) The size of the circles indicates the percentage of the deregulated genes, and the colour intensity indicates the significance (Bonferroni corrected p-value). The complete tables of enriched GO terms are in Fig. S5.

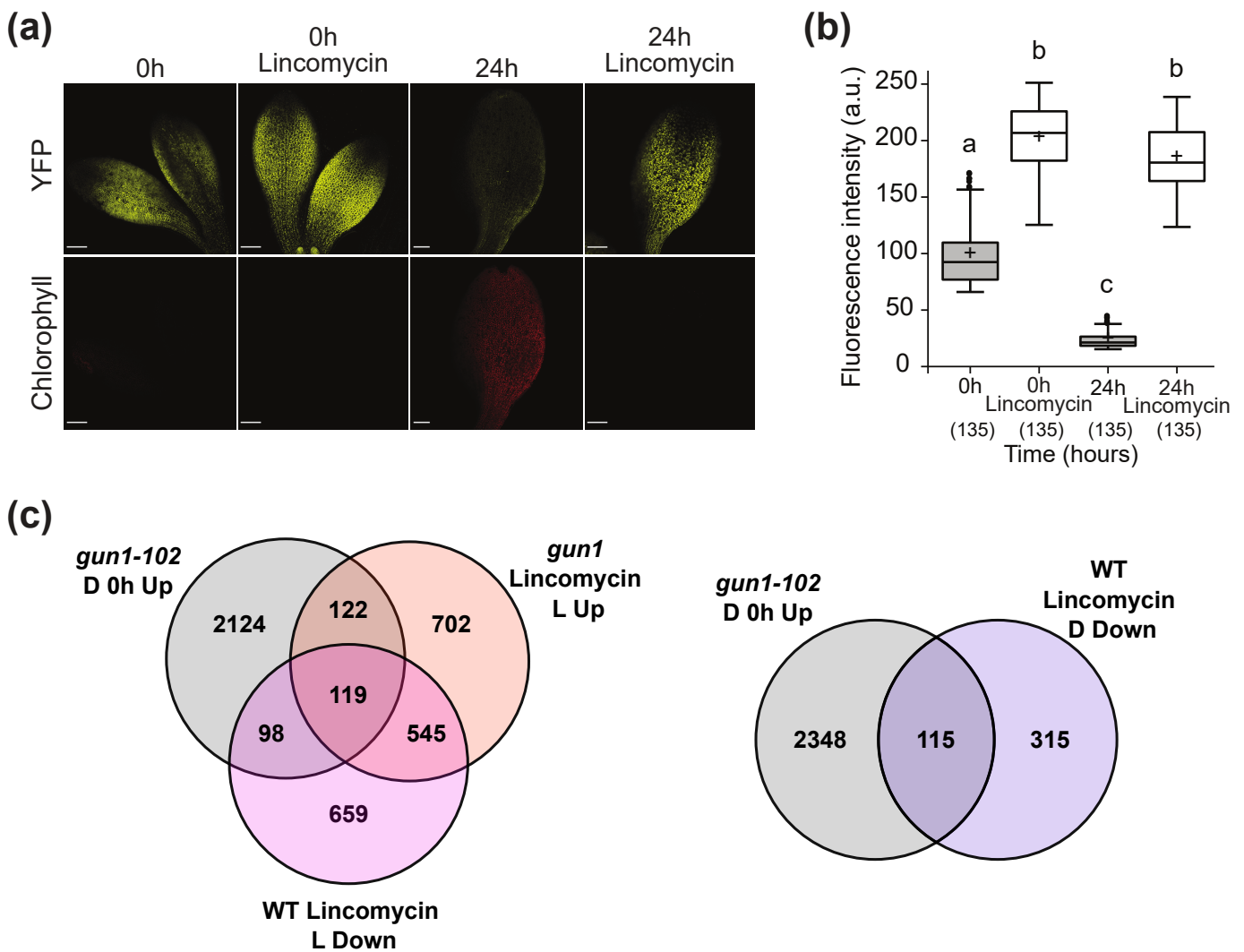


Fig. 5. GUN1:YFP response to lincomycin and comparison of etiolated *gun1-102* DEGs with *gun1* or WT Arabidopsis seedlings treated with lincomycin. (a) Fluorescence of GUN1:YFP in 5d-old etiolated cotyledons of *gun1-103 GUN1:YFP #6.3.6* seedlings grown with or without lincomycin and exposed 0 or 24h to light. Bar = 100 μ m. (b) Quantification of GUN1:YFP based on fluorescence intensity (arbitrary units; a.u.) in plastids seedlings grown as in (a). Results from three independent replicates, with 3 cotyledons per replicate and time point, and 15 chloroplasts per cotyledon (total n in brackets). Box-plot center lines show the medians and plus show the mean of all the fluorescence intensity measurements; box limits indicate the 25th and 75th percentiles; whiskers extend 1.5 times the interquartile range from the 25th and 75th percentiles; potential outliers are plotted as circles. Significance of the differences and differences between groups were determined with a Kruskal-Wallis test, $p < 2.2e^{-16}$, and a post-hoc Dunn's test with Bonferroni correction. Groups sharing a letter do not differ significantly ($\alpha = 0.05$). (c) Venn diagrams show the overlaps between *gun1-102* up-regulated DEGs in etiolated seedlings (D 0h Up) and *gun1* up-regulated DEGs in seedlings grown with lincomycin in light (Lin L Up) or WT down-regulated DEGs in seedlings grown with lincomycin in light (Lin L Down) or dark (Lin D Down).

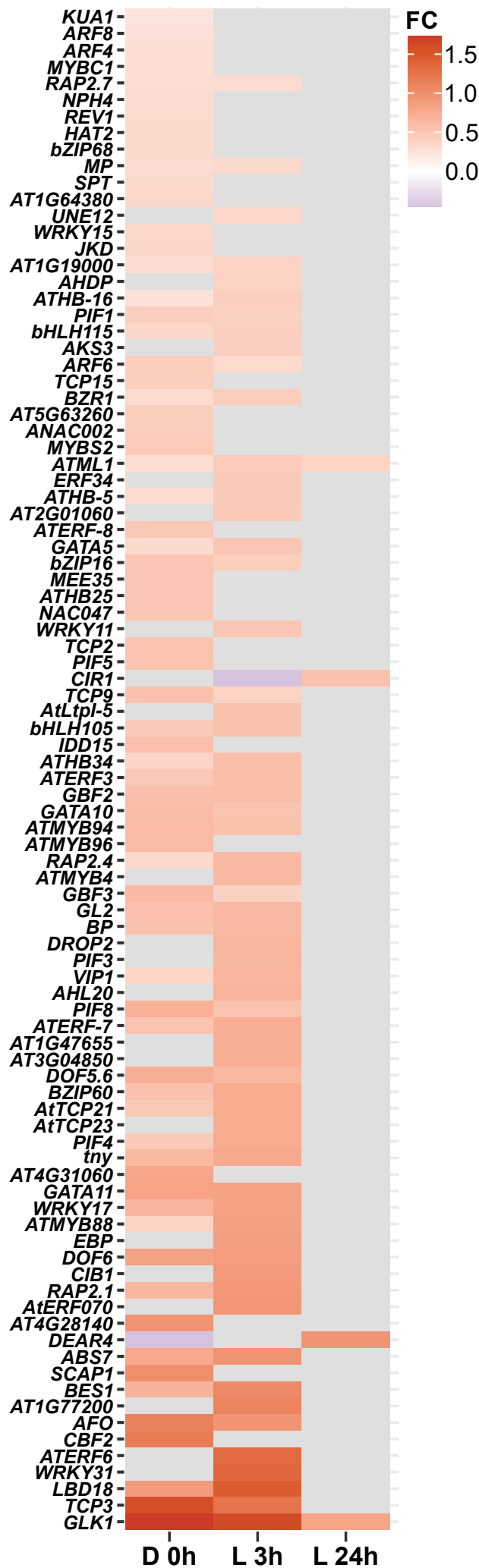


Fig. 6. Up-regulated transcription factors in *Arabidopsis gun1-102*. Heatmap of the 92 up-regulated transcription factors in *gun1-102* with potential targets among the DEGs according to TF2Network.

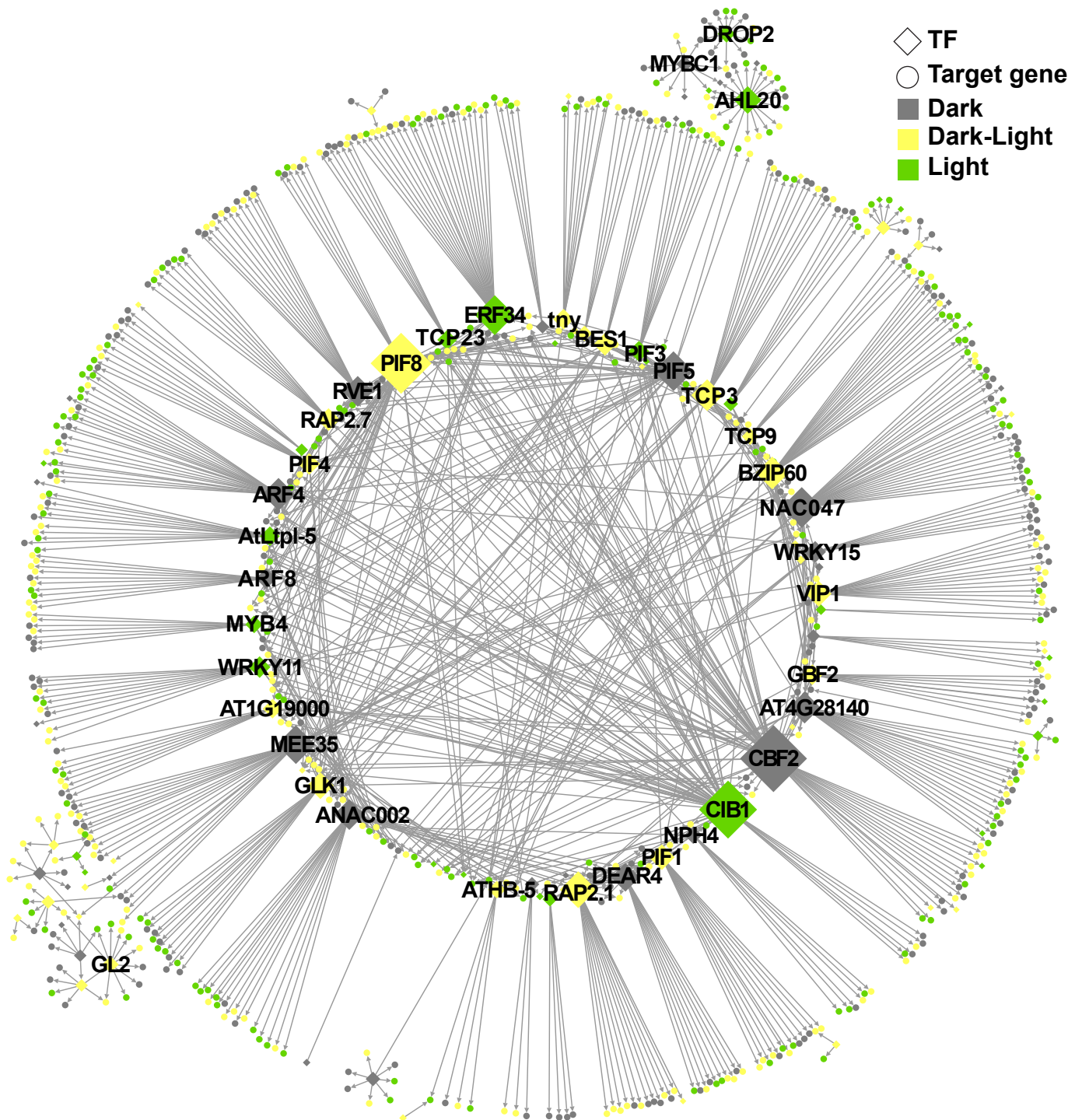


Fig. 7. Gene regulatory network (GNR) of up-regulated TFs. GRN representation of predicted regulatory interactions of 79 up-regulated Arabidopsis TFs and their respective DEGs targets are represented. Positive co-expression values and motifs overrepresented on promoters of target DEGs were considered to create regulatory interactions. Only the main connected component is represented. Sizes of TF nodes are proportional to the number of connections. A file with the network information is available in table S7.

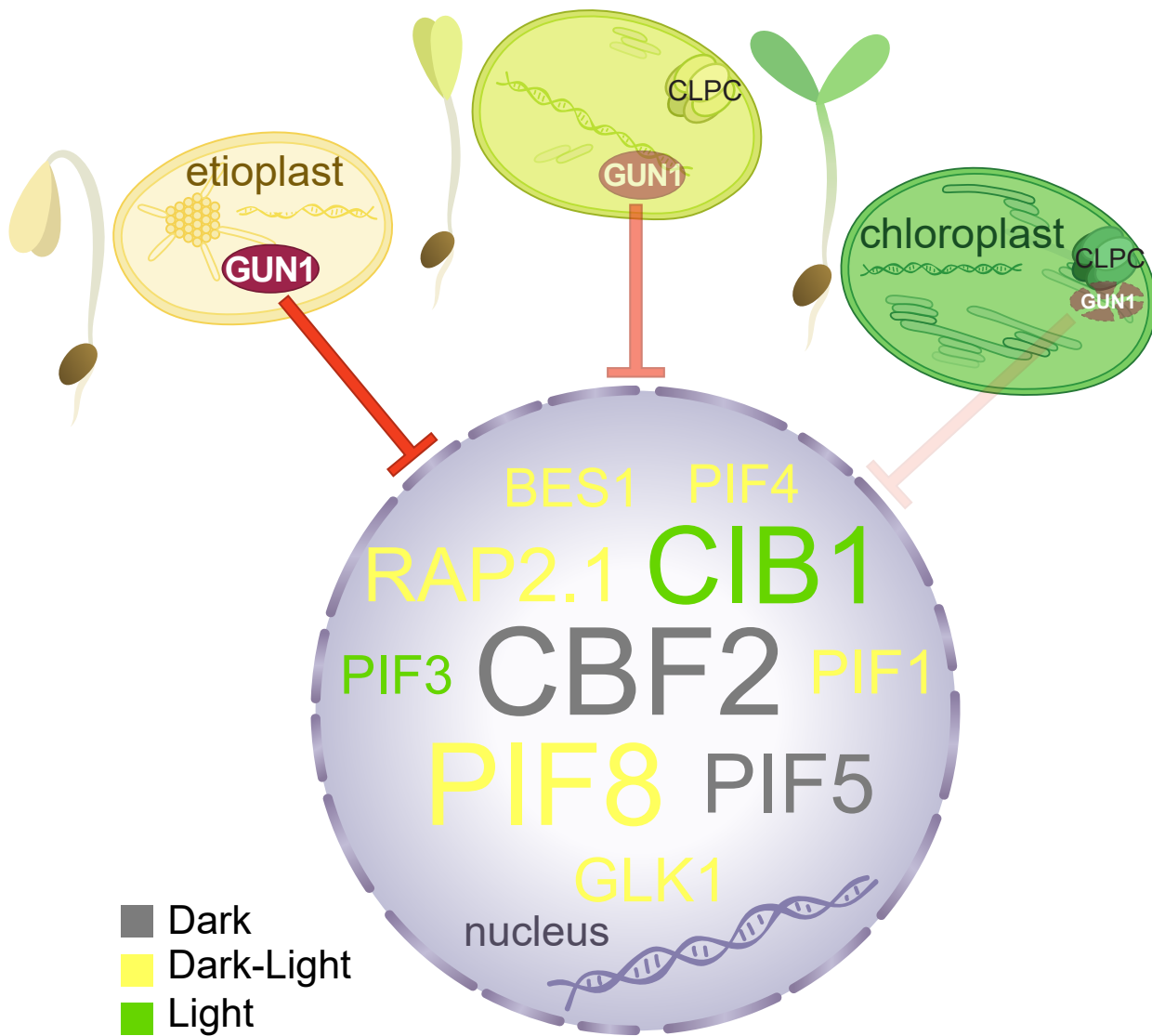


Fig. 8. Working model for GUN1 during chloroplast biogenesis in Arabidopsis. GUN1 is present in proplastids and etioplasts giving rise to a retrograde signal that regulates a large number of critical TFs linked to light response, photomorphogenesis, and chloroplast development, and consequently their downstream genes. As the light response proceeds, GUN1 levels decrease through CLPC degradation, the regulation of TFs and their downstream genes is released, transcription of *PhANGs* is boosted and the establishment of fully functional chloroplasts is achieved. In the nucleus are depicted representative GUN1-regulated TFs, repressed only in etiolated seedlings (grey), in etiolated and de-etiolated seedlings (yellow), and only in de-etiolated seedlings (green). Sizes of TFs are relative to their amount of connections in the GRN (Fig. 7 and Table S7).